Cancer Biol Med 2025. doi: 10.20892/j.issn.2095-3941.2025.0040

ORIGINAL ARTICLE

GPRC5A/CXCL8/NLRP3-mediated neutrophil extracellular traps drive gemcitabine-nab-paclitaxel resistance in pancreatic adenocarcinoma

Tianyi Zhu[1]*, Qianwen Yang[1]*, Xiaozhe Qian[2]*, Xiuqi Wu[1], Jianchen Fang[3], Yuli Lin[4,5], Yukuan Feng[6], Jian Gao[7], Qing Xia[1]

[1]Department of Oncology, Renji Hospital, Shanghai Jiao Tong University School of Medicine, Shanghai 200127, China; [2]Department of Thoracic Surgery, Renji Hospital, Shanghai Jiao Tong University School of Medicine, Shanghai 200127, China; [3]Department of Pathology, Renji Hospital, Shanghai Jiao Tong University School of Medicine, Shanghai 200127, China; [4]Center for Medical Research and Innovation, Shanghai Pudong Hospital, Shanghai 200030, China; [5]Department of Immunology, Basic Medical School, Shanghai Medical College, Fudan University, Shanghai 200030, China; [6]Department of Pancreatic Cancer, Tianjin Medical University Cancer Institute and Hospital, National Clinical Research Center for Cancer, Tianjin's Clinical Research Center for Cancer, Key Laboratory of Cancer Prevention and Therapy, Tianjin 300060, China; [7]State Key Laboratory of Systems Medicine for Cancer, Shanghai Cancer Institute, Renji Hospital, Shanghai Jiao Tong University School of Medicine, Shanghai 200032, China

ABSTRACT

Objective: Gemcitabine combined with nab-paclitaxel therapy (GnP) represents first-line chemotherapy for advanced pancreatic ductal adenocarcinoma (PDAC). However, the efficacy of GnP is diminished due to chemotherapeutic resistance induced by the tumor microenvironment (TME), the underlying mechanisms of which remain poorly understood.

Methods: Clinical data from patients with PDAC who underwent GnP therapy were collected and neutrophil infiltration in tumor tissues was assessed. PDAC cell lines and a mouse model of PDAC were utilized to determine the mechanisms underlying GnP resistance and to focus on tumor-associated neutrophils and neutrophil extracellular traps (NETs).

Results: GnP therapy recruited neutrophils to the TME, which resulted in the formation of NETs that contributed to therapeutic resistance in the PDAC murine model. The NET inhibitor, PAD4, enhanced the efficacy of GnP by suppressing tumor growth. Furthermore, GnP significantly upregulated CXCL8 secretion in GnP-resistant MIA PaCa-2 cells, which was mediated by increased expression of GPRC5A in PDAC cells. Screening of classic NET-derived molecules identified cell-free DNA (cfDNA) as a pleiotropic factor that promoted tumor cell proliferation and migration and thereby contributed to chemotherapeutic resistance. *In vivo* experiments revealed that the combination of GnP with siGPRC5A or DNase was more effective in reducing tumor growth and prolonging survival in PDAC-bearing mice than either treatment alone.

Conclusion: The GPRC5A-CXCL8-NET-cfDNA axis has a critical role in the development of therapeutic resistance to GnP in PDAC. Targeting this axis may represent a promising strategy for overcoming GnP resistance and thereby enhancing the efficacy of chemotherapy in PDAC.

KEYWORDS Pancreatic ductal adenocarcinoma; GnP resistance; neutrophil extracellular traps; GPRC5A; tumor microenvironment

Introduction

Pancreatic ductal adenocarcinoma (PDAC) is the most prevalent form of pancreatic cancer and comprises > 90% of cases[1]. Current treatment options for PDAC include surgery, radiation, chemotherapy, and targeted therapy[2]. Despite surgical intervention, the 5-year survival rate is approximately 11%[3]. Greater than 80% of patients with PDAC experience relapse that necessitates adjuvant chemotherapy[2,4]. Gemcitabine combined with nab-paclitaxel (GnP) has demonstrated superior

*These authors contributed equally to this work.
Correspondence to: Yuli Lin, Yukuan Feng, Jian Gao and Qing Xia
E-mail: yulilin@fudan.edu.cn, fengyukuan@tjmuch.com, lumenhj1937@163.com and xiaqing@shsmu.edu.cn
ORCID ID: https://orcid.org/0000-0002-8779-2471, https://orcid.org/0009-0005-6497-0748, https://orcid.org/0000-0002-2830-4810 and https://orcid.org/0000-0002-7001-5908
Received February 6, 2025; accepted June 3, 2025;
published online July 15, 2025.
Available at www.cancerbiomed.org
©2025 The Authors. Creative Commons Attribution-NonCommercial 4.0 International License

survival outcomes compared to monotherapy with either gemcitabine or nab-paclitaxel in a phase III clinical trial[5]. Another multicenter clinical trial focusing on postoperative PDAC reported a 5-year survival rate of 36% with GnP treatment[4]. Although GnP is one of the first-line therapies for advanced PDAC[6], the objective response rate is only approximately 20%[5]. Most patients will be confronted with disease progression after a short period and the development of therapeutic resistance persists, potentially due to complex interactions with the tumor microenvironment (TME) in PDAC[7].

The TME in PDAC consists of various cell types; neutrophils are abundant and have crucial roles in tumor progression[8,9]. Like M1 and M2 for macrophages, some studies have divided tumor-associated neutrophils (TANs) into two populations (antitumor N1 and protumor N2 neutrophils)[10]. A wide spectrum of neutrophil states has been identified with differences in gene expression[11,12] and suggests the intricacy of neutrophil function in PDAC. Ejection of neutrophil extracellular traps (NETs), which are web-like DNA structures decorated with histones and granule proteins, is one of the complicated roles of neutrophils[13]. Patients with PDAC and high neutrophil infiltration and positive NET staining have poorer progression-free survival (PFS) and disease-specific survival (DSS). NET formation is an independent prognostic factor for DSS[14]. In addition, patients with PDAC and low neutrophil infiltration or negative NET staining are more likely to benefit from 5-fluorouracil- and/or gemcitabine-based chemotherapies[14]. A high neutrophil-to-lymphocyte ratio (NLR) in peripheral blood is a prognostic factor for poor survival in patients with PDAC[15,16]. Reduction of NETs resulted in delayed tumor growth and improved survival in mouse models of orthotopic pancreatic adenocarcinoma[17]. NET inhibitors, such as GSK484, DNase I, or antagonists of chemotactic receptors CXCR1/CXCR2, inhibit tumor progression[17]. Furthermore, NETs promote tumor proliferation by activating pancreatic stellate cells, while removal attenuates tumor growth[18].

NETs can affect the biological behavior of tumor cells, while tumor cells induce NET formation[19]. Cytokines secreted in the tumor microenvironment, including CXCL8[20,21], TIMP-1[22], IL-17[23], G-CSF[24,25], TGF-β[26], and IL-13[27] have been shown to induce NET formation. Breast cancer cells are also capable of stimulating NETs and thereby enhance cancer cell mobility[28]. In addition, some chemotherapeutic agents, such as cisplatin or adriamycin/cyclophosphamide, promote NET formation in breast cancer lung metastasis[19]. Oxaliplatin induced NETs in a mouse model; targeting NETs is a potential strategy for treating oxaliplatin-induced peripheral neuropathy[29]. However, the effect of GnP on NETs in PDAC has not been established.

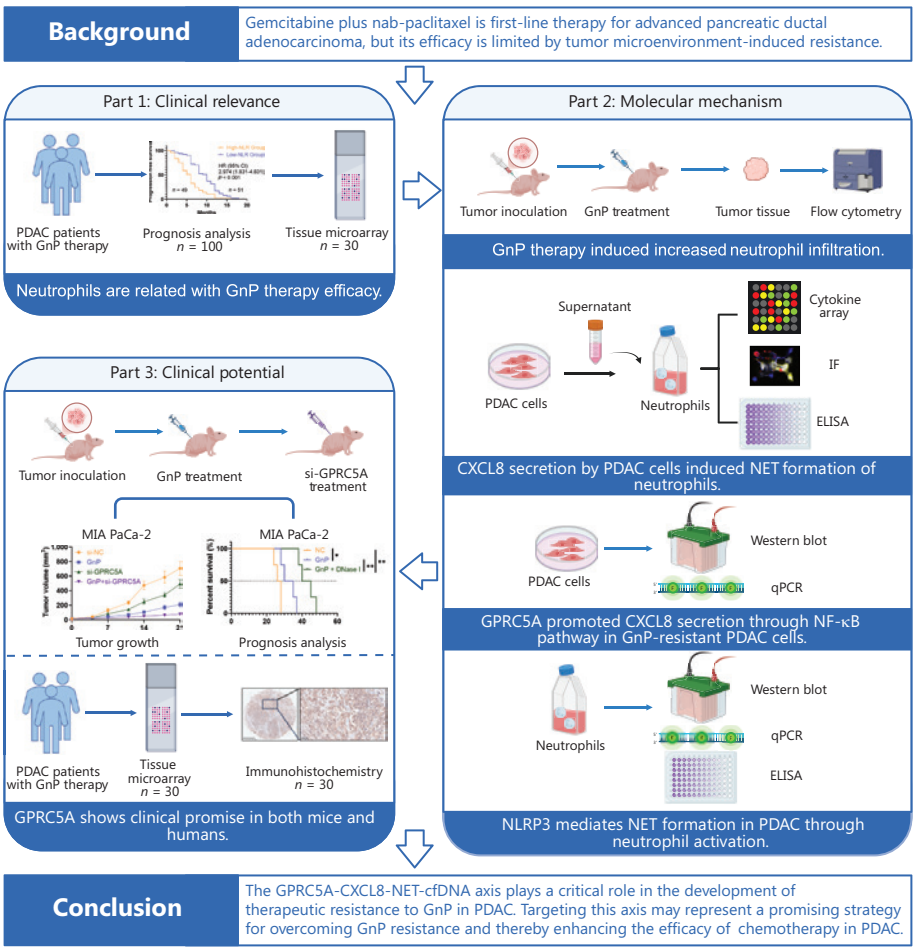
G protein-coupled receptor class C group 5 member A (GPRC5A) is an orphan receptor coupled to G proteins and exhibits dual behavior in cancer. GPRC5A knockout mice spontaneously develop lung cancer. Normal lung tissue has a higher level of GPRC5A expression than tumor tissues, which suggests that GPRC5A has a tumor-suppressing function[30]. Similarly, GPRC5A inhibits IL-6-induced STAT3 activation and represses the growth of head and neck squamous cell carcinoma[31]. Conversely, GPRC5A acts as a proto-oncogene because GPRC5A overexpression restores the growth of pancreatic cancer suppressed by miR-135b-5p inhibition[32]. GPRC5A is associated with chemotherapy resistance in pancreatic cancer[33,34] but the precise mechanism has not been established.

In the current study GnP was shown to induce neutrophil recruitment and NET formation, which reduces the therapeutic response in mouse models of PDAC. GnP treatment enhanced PDAC cells to secrete CXCL8 by increasing GPRC5A expression. As a result, CXCL8 triggered NET formation by increasing the NLR family pyrin domain containing 3 (NLRP3) level. NET-derived cell-free DNA (cfDNA) has a crucial role in conferring chemoresistance by promoting tumor cell proliferation and migration. Moreover, GnP and si-GPRC5A combination therapy had a significant therapeutic effect compared to monotherapy. Thus, the GPRC5A-CXCL8-NET-cfDNA axis contributes to GnP chemoresistance in PDAC (**Study flow chart**).

Materials and methods

Cell culture

MIA PaCa-2, PANC-1, and HL-60 cell lines were purchased from Wuhan Pricella (Wuhan, China). MIA PaCa-2 and PANC-1 were cultured in Dulbecco's Modified Eagle's Medium [DMEM] (Gibco, Thermo Fisher Scientific, Waltham, MA, USA), and HL-60 in Iscove's Modified Dulbecco's Medium [IMDM] (Gibco), both of which were supplemented with 10% FBS (HyClone Laboratories, Cytiva, Logan, UT, USA), 100 U/mL of penicillin (Yeasen, Shanghai, China), and 100 μg/mL of streptomycin (Yeasen, Shanghai, China) at 37°C in 5% CO_2. All cells were *Mycoplasma*-negative at the last passage. A co-culture system of bone-marrow-derived neutrophils (BMDNs) with MIA PaCa-2 or PANC-1 cells was established. MIA PaCa-2 or PANC-1 cells were cultured in 10 cm-diameter dishes (Corning, NY, USA) and 3×10^5/mL



Study flow chart GPRC5A-CXCL8-NET-cfDNA axis contributes to chemotherapy resistance in pancreatic ductal adenocarcinoma. Part 1 illustrates tissue microarray and prognosis analysis of PDAC patients undergoing GnP therapy revealed that neutrophil levels were associated with treatment outcomes. Part 2 shows that in murine models, GnP therapy increased neutrophil infiltration in tumors. Conditioned medium from PDAC cells promoted neutrophil extracellular trap (NET) formation through CXCL8 secretion. Mechanistically, GPRC5A enhanced CXCL8 secretion *via* NF-κB signaling in GnP-resistant PDAC cells, while NET formation was mediated by NLRP3 activation in neutrophils. Part 3 presents that inhibition of GPRC5A in PDAC-bearing mice reduced tumor growth and improved survival under GnP therapy, highlighting the therapeutic potential of targeting GPRC5A. *, $P < 0.05$; **, $P < 0.01$ (created with biorender.com).

freshly separated mouse-derived neutrophils were added to the media when the tumor cells reached 80% confluence. HL-60 cells were induced to mature neutrophils by incubating with 1% DMSO (Sigma-Aldrich, St. Loui, MO, USA) and 5 μM all-trans-retinoic acid (ATRA) (MCE, MedChemExpress, Monmouth Junction, NJ, USA) for 5 d. Giemsa staining was performed to verify the maturation of neutrophils.

GnP treatment was introduced to the culture media at different concentrations to induce GnP resistance in MIA PaCa-2 and PANC-1 cells. GnP was added to the media and cultured for 24 h when the tumor cells reached 60%–80% confluence. The cells were then rinsed twice with PBS and returned to normal media until the typical morphology was exhibited. This process was repeated until the tumor cells could grow steadily in the presence of GnP. The most effective concentration was evaluated and confirmed using the CCK8 assay. The working concentrations for MIA PaCa-2 and PANC-1 were 1 μM gemcitabine + 0.68 μM nab-paclitaxel and 9.5 μM gemcitabine + 1.9 μM nab-paclitaxel, respectively.

Human samples and mouse models

Human PDAC specimens were obtained from Renji Hospital affiliated with Shanghai Jiao Tong University School of

Medicine (Shanghai, China). The study was conducted according to the Declaration of Helsinki. All tissues and experiments were reviewed and approved by the Ethics Committees of Renji Hospital (Approval Nos. KY2020-116, KY2024-059-C). Clinical data were collected and anonymized before analysis. A total of 152 patients with PDAC were initially enrolled in this study. Of the 152 patients, 42 who received treatment regimens other than GnP were excluded from analyses focusing on treatment efficacy. An additional 10 patients who were lost to follow-up were excluded. As a result, 100 patients were included in the Kaplan–Meier survival analysis and in the evaluation of the NLR as a predictor of treatment response. Tumor specimens were only available from a subset of patients for immunofluorescence (IF) staining of CD66b and immunohistochemistry (IHC) staining of GPRC5A. Due to limited access to resected tumor tissues, 70 patients lacked suitable samples for staining. Therefore, a total of 30 tumor specimens were included in the IF analysis. The median was taken as the cut-off value in survival analysis. Thirty PDAC surgical samples were collected between 2020 and 2023; the clinical characteristics are listed in **Table S1**. The responsive group was defined as patients with a complete response plus partial response after two cycles of chemotherapy treatment when assessing treatment efficacy. The non-responsive group was defined as progressive disease.

All animal experiments were approved by the Institutional Animal Care and Use Committee of the Animal Core Facility of the Shanghai Jiao Tong University School of Medicine Affiliated Renji Hospital (Approval No. RJ2022-0811). All performances adhered to local and national requirements for the care and use of laboratory animals. Five-week-old female BALB/c-nude mice were randomly distributed into groups and anesthetized to generate the subcutaneous PDAC model. MIA PaCa-2 cells were dissociated and injected subcutaneously into the mice (5×10^6 cells in 100 μL DMEM). Treatment started 1 week after injection of PDAC cells. The tumor-bearing mice were treated intraperitoneally with gemcitabine (100 mg/kg) together with albumin-paclitaxel (20 mg/kg) and/or anti-Ly6G (RRID: AB_1107721; Bio X Cell, West Lebanon, NH, USA). Mice were injected intraperitoneally with GnP as described above to assess small interfering (si)RNA treatment efficacy and treated with si-NC (5 nmol/20 g) or si-GPRC5A (5 nmol/20 g; Ribobio, Guangzhou, China) intratumorally twice per week for 3 weeks. The size of the tumors was measured twice per week and when the tumor volume reached approximately 800 mm^3 or at the time mice were sacrificed. All mice were housed in SPF barrier facilities.

Flow cytometry

Subcutaneous tumors were collected, minced, digested, and strained through a 70-μm nylon filter for single-cell suspensions. The cells were first incubated for 15 min with anti-CD16/CD32 antibody (#14-0161-82, 1:300; eBioscience) to block Fc receptors, then primary antibodies for 45 min on ice. The primary antibodies included CD45, F4/80, Ly6G,CD11b, CD11c, and NK1.1, which were used to label macrophages, neutrophils, dendritic cells, and natural killer cells. The antibodies used are listed in **Table S2** (Supporting Information). Data were collected using a flow cytometer (BD LSRFortessa™ X-20) and analyzed using FlowJo software (Tree Star, Ashland, OR, USA).

Isolation of neutrophils

Mice were sacrificed and the femurs were collected and flushed using a sterile syringe filled with 1 × PBS, then collected into a sterile 50-mL tube. The bone marrow cells were collected by centrifugation at 400 × *g* for 5 min, then suspended in PBS. An EasySep™ Mouse Neutrophil Enrichment kit (Stemcell, Technologies, Vancouver, BC, Canada) was used to purify BMDNs. After centrifugation and resuspension, the remaining cells were collected as neutrophils and assessed for purity and viability by Giemsa and trypan blue staining, respectively.

NETosis assay

BMDNs or HL-60-derived neutrophils were seeded in 96-well plates at a density of 3×10^5 cells/mL and treated with DMEM (media group), GnP-resistant MIA PaCa-2 or PANC-1 cell culture medium [conditioned media (CM) group], or LPS (100 ng/mL), or untreated (blank group). The MPO-DNA complexes were detected according to a previous study[35]. Anti-MPO antibody (Cayman, Chemical, Ann Arbor, MI, USA) was used as a capture antibody and a peroxidase-labeled anti-DNA primary antibody (Cell Death Detection Enzyme-linked Immunosorbent Assay kit; Roche, Basel, Switzerland) was used as the detection antibody. Equal volumes of plasma or neutrophil supernatant were subjected to MPO-DNA ELISA. The MPO activity of neutrophils was performed using a Neutrophil Myeloperoxidase Activity Assay kit (Cayman).

The cfDNA was quantified with a Quant-iT PicoGreen dsDNA Assay kit (Thermo Fisher Scientific, Waltham, MA, USA). All procedures were performed according to the manufacturer's instructions.

Transwell cell migration assay

Transwell migration assays were performed as previously described[36]. The culture medium of GnP-resistant PANC-1 cells was collected, centrifuged at 450 g for 5 min and filtered through a 0.45-μm membrane. The filtered culture medium was added to the mouse BMDNs with or without GSK484 (10 μM; MCE). The neutrophil culture medium supernatant was collected after 4 h and added to PANC-1 cells with or without GnP. Approximately 2×10^4 PANC-1 cells were added to an 8-μm pore size Transwell chamber in a 24-well plate 24 h earlier. Media containing 10% FBS were plated into the bottom chamber. After incubation for 24 h, the cells were fixed and dyed with methanol and crystal violet, respectively. Migrated cells were counted in five randomly selected fields using a microscope. The assays were run in triplicate.

CCK-8 cell viability assay

The NET inhibitor, GSK484 hydrochloride, was added to the co-culture system described above to assess the effect of NETs on PDAC cell resistance to GnP therapy. The culture media were collected and added to GnP-resistant MIA PaCa-2 or PANC-1 cell culture dishes. MIA PaCa-2 and PANC-1 cells were dissociated and seeded in 96-well plates at a density of 3,000 cells per well and incubated overnight. Cell viability (OD450) was measured after reacting with a Cell Counting Kit-8 [CCK-8] (MCE) for 2 h.

Western blot

Cells were collected and washed twice with cold PBS and lysed with proteinase inhibitor on ice. The suspension was collected after centrifugation at 14000 g for 15 min at 4°C. The suspension was collected as total protein and the concentration was measured using a BCA Protein Assay kit (Thermo Fisher Scientific). Equal amounts of proteins were added on SDS-page gels for separation, transferred to PVDF membranes (Millipore, Billerica, MA, USA), and blocked with 5% BSA at room temperature for 1 h. The membranes were incubated overnight with primary antibodies at 4°C and thrice-washed with TBST, followed by 1-h incubation with secondary antibodies at 37°C. Protein bands were visualized using a chemiluminescence detection system. The antibodies that were used are listed in **Table S2** (Supporting Information). Western blot bands were quantitatively analyzed using Image J software (National Institutes of Health, Bethesda, MD, USA).

Subcellular fractionation

Fractionation of nuclear and cytosolic extracts was performed using the Nuclear and Cytoplasmic Protein Extraction kit (catalog no. P0027; Beyotime, Beijing, China) according to the manufacturer's instructions.

IF

The paraffin-embedded samples were sectioned and deparaffinized. Antigen retrieval was performed using citrate-EDTA buffer at 100°C for 30 min. The slides were then rinsed in ddH_2O and blocked in 2% BSA, goat serum, and 3% Tx-100 for 30 min at room temperature, and incubated in primary antibody overnight at 4°C. Antibody information is provided in **Table S2** (Supporting information). The slides were thrice-washed in TBST and incubated with secondary antibodies for 30 min at room temperature. The slides were then rinsed, cover-slipped, and imaged on an Andor Dragonfly (CD-DFLY-505; Andor Technology Ltd., Belfast, Northern Ireland, UK). CD66b and GPRC5A expression was determined by a pathologist using ImageJ for quantification.

PANC-1 cells were transfected with si-GPRC5A or si-NC using the Hieff Trans® Liposomal Transfection reagent (40802ES03; Yeasen, Shanghai, China) following the manufacturer's instructions. The transfection efficiency was assessed *via* qPCR. The transfected PANC-1 cells were subsequently treated with 9.5 μM gemcitabine and 1.9 μM nab-paclitaxel for 24 h, then the conditioned media were collected separately. BMDNs were collected as previously described, then incubated with the conditioned media from GPRC5A-knockdown PANC-1 cells or the control group for 24 h. The treated BMDNs were fixed with 4% paraformaldehyde at 4°C overnight, permeabilized, and blocked after culture, then incubated with primary antibody against MPO, citH3, and CD66b for 1 h at 37°C. The antibody details are listed in **Table S2**. Then, the cells were incubated with secondary antibodies and DAPI, and imaged as outlined above.

IHC

Tissue microarray containing the collected 30 PDAC tissues was subjected to immunohistochemical analysis using an anti-GPRC5A antibody (**Table S2**) to determine GPRC5A expression. IHC was performed according to the manufacturer's instructions (PK10006; Proteintech, Wuhan, China). Quantitative analysis of GPRC5A staining was performed as previously described[37].

Cytokine array

Cytokine array allowing simultaneous detection of cytokines was used to assess secretion profiles in CM from GnP-resistant MIA PaCa-2 cells according to the manufacturer's instructions. Cytokine array was performed by RayBiotech (AAH-CYT-1000; Guangzhou, China).

ELISA-based quantification of cytokines

Cell culture supernatants of GnP-resistant MIA PaCa-2 or PANC-1 cells were collected to evaluate CXCL8. CXCL8, TNF-α, IL-12, IL-1Ra, TGF-β1, and elastase secretion. ELISA kits (RayBiotech) were used according to the manufacturer's instructions. Each sample was run in triplicate.

RNA isolation and quantitative reverse transcription (qRT-PCR)

Total RNA was extracted using TRIzol reagent for real-time qRT-PCR following the manufacturer's instructions. RNA samples were reverse-transcribed into cDNA using a cDNA synthesis kit (Takara, Tokyo, Japan). The qRT-PCR was performed using a SYBR Green Master Mix kit (Roche) in QuantStudio 7 Flex (AppliedBiosystems, Thermo Fisher Scientific). The results were standardized to GAPDH values. The primers used for key genes are as follows: GPRC5A (F: 5′-ATGGCTACAACAGTCCCTGAT-3′; R: 5′-CCACCG TTTCTAGGACGATGC-3′); NF-κB p65 (F: 5′-ACCGCTGC ATCCACAGTTTC-3′; R: 5′-GGGGTTGTTGTTGGTCTGG A-3′); CXCL8 (F: 5′-ACTGAGAGTGATTGAGAGTGGAC-3′; R: 5′-AACCCTCTGCACCCAGTTTTC-3′); and GAPDH (F: 5′-GGAGCGAGATCCCTCCAAAAT-3′; R: 5′-GGCTGTT GTCATACTTCTCATGG-3′). Primer sequences for other genes are listed in **Table S3**. The sequences for siRNA use in inhibiting GPRC5A *in vitro* were as follows: siGPRC5A (5′-AGGCAGCAUUUUUCGCCUGTT-3′); and si-NC (5′ GUAGAUUACCACUGGAGUCTT-3′). The sequences for GPRC5A-siRNA *in vivo* were si-h-GPRC5A_001 [2Ome+5Chol] (5′-AGGACTCCAACAGGCGAAA-3′) from RIBOBIO.

Statistical analysis

All experiments were performed at least three times. Statistical analysis was performed using Prism software (GraphPad Software, Inc., La Jolla, CA, USA). The unpaired Student's *t*-test and Mann–Whitney *U* test were used for comparison between the two groups depending on the distribution. One- and two-way ANOVA were used for comparisons between three or more groups. The log-rank test (survival) was used to determine statistical significance. The sample size for survival analysis was estimated based to be 82 patients based on an expected hazard ratio of 2.0 with an $\alpha = 0.05$ and a power = 80%. A $P < 0.05$ was considered significant for all comparisons.

Results

Neutrophil infiltration is associated with poor prognosis in patients treated with GnP therapy

Clinical data from 100 patients with complete follow-up records in the Shanghai Jiao Tong University School of Medicine Affiliated Renji Hospital were collected to assess the effect of neutrophils on pancreatic cancer patients (**Figure 1A**, **Table S1**). A high NLR is a prognostic factor for poor PFS in patients with unresectable PDAC treated with gemcitabine[38]. The NLRs of patients with resected PDAC were calculated at the time of admission to Renji Hospital for surgery. The survival analysis indicated that a high NLR was correlated with reduced PFS (**Figure 1B**). Additionally, patients with a poor response to GnP therapy had a significantly elevated NLR (**Figure 1C**). CD66b staining was performed to further validate neutrophil infiltration in PDAC tissues. The results revealed that patients with high CD66b expression had a worse prognosis (**Figure 1D and 1E**).

GnP recruits neutrophils and promotes NETosis in the PDAC

MIA PaCa-2 cells were injected subcutaneously into BALB/c-nude mice to establish a PDAC model. The model was used to

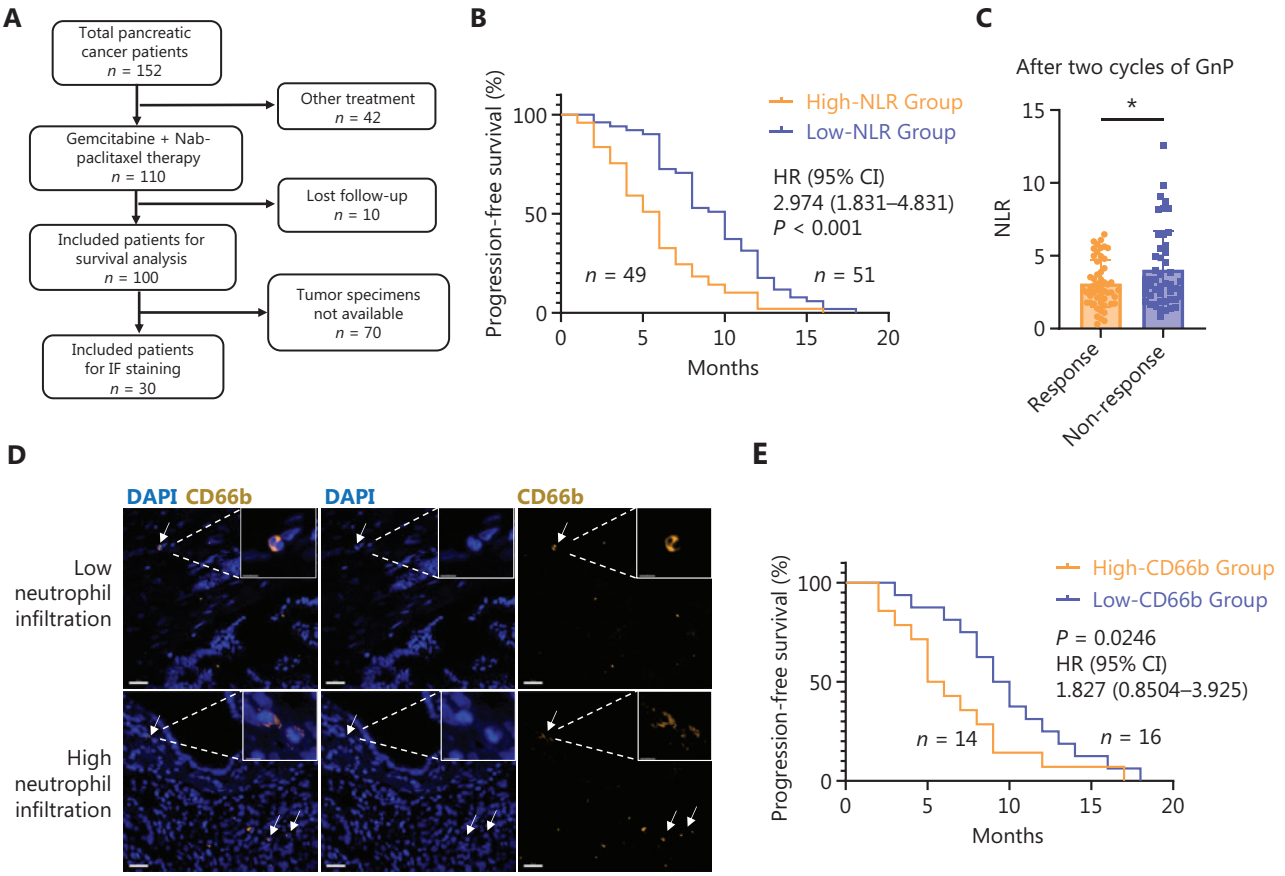


Figure 1 Clinical correlation of neutrophil infiltration and PDAC prognosis. (A) Schemes for the collection of patient information and human PDAC samples. (B) Kaplan–Meier plots of the progression-free survival (PFS) of patients with PDAC with a high neutrophil-lymphocyte ratio (NLR) and low NLR. The cut-off value was the NLR median (n = 100). The medians PFS of the low and high NLR groups were 10 and 5.5 months, respectively. (C) NLR level between GnP-responsive and -non-responsive patients after two GnP treatment cycles (n = 100). The responsive group included patients with complete and partial responses. The non-responsive group included patients with progressive disease. (D) Representative images of human PDAC patient samples for CD66b (yellow) and DAPI (blue). White arrows point to neutrophils. The cut-off value is the CD66b MFI median. Scale bar, 30 μm. (E) Kaplan–Meier plots of the PFS of patients with PDAC with high and low CD66b and expression (n = 30). The cut-off value was the CD66b MFI median (n = 30). The median PFS of low and high CD66b levels was 10.5 and 7.0 months, respectively. The P value shown was determined by the log-rank test in (B) and (E). Unpaired t-test was used in (C)*, $P < 0.05$. Data are the mean ± SD.

determine how GnP modifies the TME in PDAC. Tumor formation was observed after 7 days. The mice were then treated intraperitoneally with GnP chemotherapy [gemcitabine (100 mg/kg) and nab-paclitaxel (20 mg/kg)] twice a week for 21 d before being sacrificed. A single-cell suspension was prepared from tumor tissues, and the percentage of macrophages, neutrophils, dendritic cells, and natural killer cells was quantified using flow cytometry to determine the effect of GnP therapy on the tumor immune microenvironment (**Figure S1**). A significant increase in neutrophils was noted in GnP-treated tumors, whereas other immunocytes were not significantly affected by GnP treatment (**Figure 2A**). Because of the marked increase in neutrophil infiltration, whether GnP therapy influenced neutrophil chemotaxis was determined. To evaluate this hypothesis, GnP was added to the neutrophil culture medium, but there was no effect on neutrophils (**Figure 2B**). All MIA PaCa-2 and PANC-1 cells were treated with GnP at different doses for 24 h before experiments were performed to establish GnP-resistant MIA PaCa-2 and PANC-1 cell lines and to determine the role of tumor cells in the significant increase of neutrophils, (**Figure S2**). CM from GnP-resistant MIA PaCa-2 and PANC-1 cancer cells enhanced neutrophil chemotaxis *in vitro* (**Figure 2C**). This outcome suggested that GnP therapy may promote neutrophil migration into PDAC tumor tissues

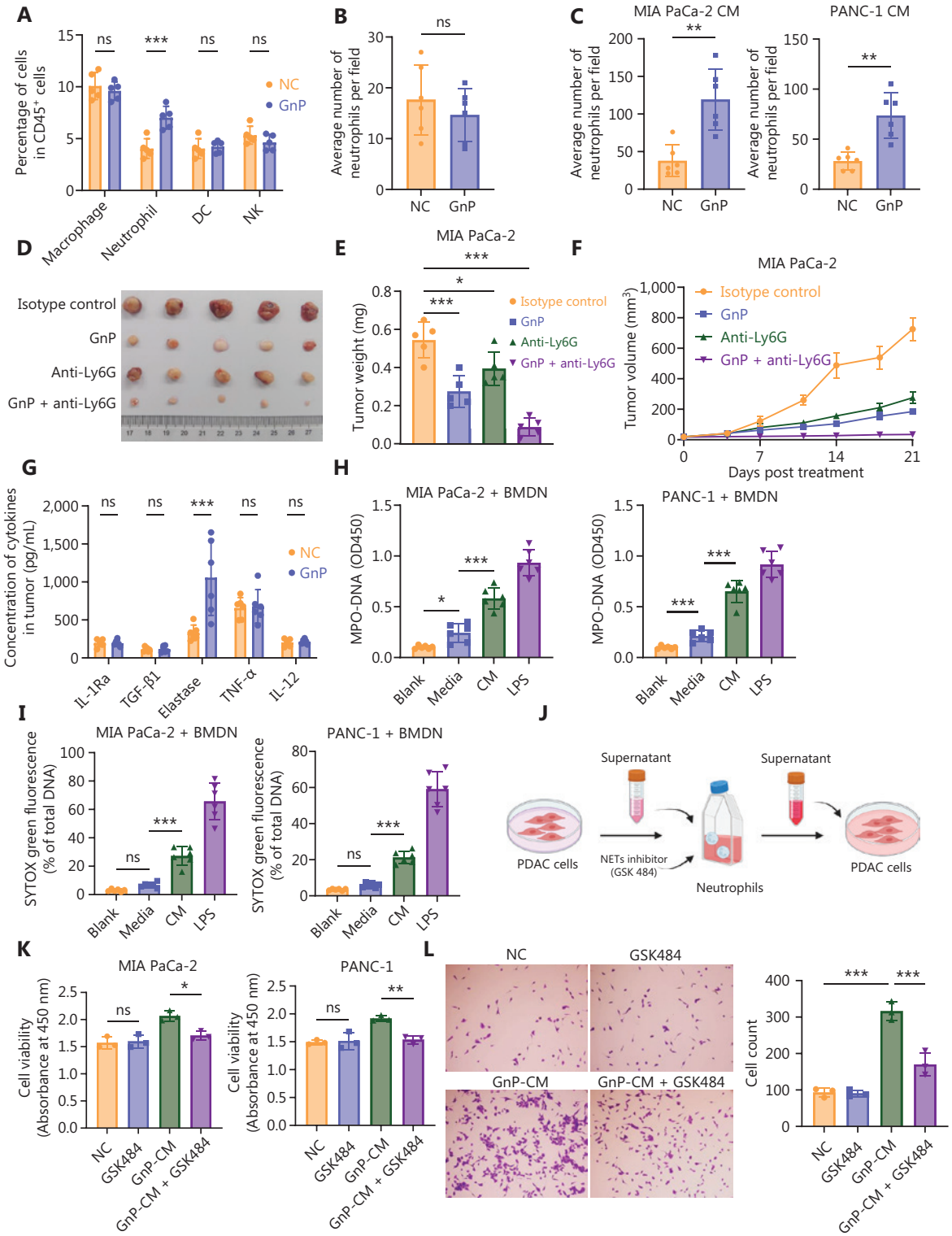


Figure 2 GnP treatment induces neutrophil infiltration and NET formation and contributes to chemoresistance in PDAC. (A) Percentage of the CD45$^+$CD11b$^+$F4/80$^+$ macrophages, CD45$^+$CD11b$^+$Ly6G$^+$ neutrophils, CD45$^+$NK1.1$^+$ natural killer cells (NK), and CD45$^+$CD11b$^+$CD11c$^+$ dendritic cells (DC) in tumor tissues of negative control (NC; n = 5 per group) and GnP-resistant MIA PaCa-2-bearing BALB/c-nude mice. (B) Measurements of the neutrophil number recruited by GnP and (C) conditioned medium (CM) of GnP-resistant MIA PaCa-2 (MIA PaCa-2 CM) and PANC-1 (PANC-1 CM) cells by microscopy. (D) Tumor photo, (E) tumor weight, and (F) tumor growth curve of MIA PaCa 2-bearing

BALB/c-nude mice that received treatments by isotype control, GnP, anti-Ly6G antibody (neutrophil depletion), or GnP + anti-Ly6G antibody when the tumor volume reached approximately 20 mm^3. (G) Measurements of neutrophil-derived cytokines using enzyme-linked immunosorbent assay (ELISA), n = 6, (H) Measurements of MPO-DNA by ELISA, and (I) the fluorescence intensity of SYTOX Green in bone marrow-derived neutrophils (BMDNs) that were not treated (blank) or treated with DMEM (media), CM from GnP-resistant MIA PaCa-2 or PANC-1 cells (CM), or LPS (100 ng/mL). (J) Diagram depicting the experimental design used in **Figure 2**. K–L (created with Biorender.com). (K) Cell viability assessed by CCK-8 assay in GnP-resistant MIA PaCa-2 and PANC-1 cells following treatment with control media (NC), conditioned media (CM) from neutrophils treated with GSK484 (100 nM), CM from neutrophils stimulated by GnP-resistant cancer cell CM, and CM from neutrophils exposed to GnP-resistant cancer cell CM in combination with GSK484 (GnP-CM + GSK484). (L) Representing images and quantification of migration of MIA PaCa-2 treated by media (NC), GSK484 (100 nM), media from GnP-resistant relative cells (GnP-CM), and GnP-CM + GSK484. All experiments were performed at least thrice. For statistical analyses, two-way ANOVA was used for (A) and (G). An unpaired t-test was used for (B) and (C). One-way ANOVA was used for (E), (H), (I), (K), and (L). *, $P < 0.05$; **, $P < 0.01$; ***, $P < 0.001$; ns, not significant. Data are the mean ± SD.

by increasing the production of some chemokines. *In vivo* experiments demonstrated that neutrophil depletion by anti-Ly6G antibody improved the effectiveness of GnP in reducing tumor volume (**Figure 2D**) and weight (**Figure 2E**) in BALB/c-nude mice. In like manner, the tumor growth (**Figure 2F**) was more effectively inhibited in mice receiving combination therapy compared to mice receiving GnP alone. These findings indicated a key role for neutrophils in mediating resistance to GnP in pancreatic cancer treatment.

Various neutrophil cytokines in tumor tissue homogenates from MIA PaCa-2-bearing BALB/c-nude mice were assessed by ELISA to further investigate the effects of GnP therapy on neutrophils. Because neutrophils synthesize and secrete pro- and anti-inflammatory factors, TNF-α, IL-12, IL-1a, TGF-β1, and elastase were selected as representative cytokines to evaluate the functional changes of neutrophils after GnP therapy. Elastase levels significantly increased following GnP therapy, whereas the other pro- and anti-inflammatory factors showed only minor changes (**Figure 2G**). Given that elastase is a NET marker, the results suggested that GnP therapy might induce NET formation in PDAC. CM from GnP-resistant MIA PaCa-2 or PANC-1 cancer cells were cultured with freshly isolated BMDNs to determine how GnP therapy influences NETs. Neutrophils formed NETs when cultured with PDAC cells but only in co-cultures treated with GnP therapy, as determined with MPO-DNA (**Figure 2H**) and SYTOX Green (**Figure 2I**). The NET inhibitor, GSK484 hydrochloride, was introduced in the co-culture system to further explore the effect of NETs on PDAC cell behavior. The CM of GnP-sensitive or resistant PDAC cells were first collected and neutrophils were treated with or without the addition of GSK484. Neutrophil CM (**Figure 2J**) were used to treat GnP-resistant PADC cells prior to the CCK-8 and Transwell assays. NET inhibition overcame GnP therapy resistance, as demonstrated by the CCK-8 (**Figure 2K**) and migration assays (**Figure 2L**). The changes in proliferation and migration induced by GnP-CM were moderate, which may reflect early adaptive responses to chemotherapy-induced secretory signals and could contribute to a more permissive microenvironment that supports residual tumor cell survival and reshape the immune environment.

CXCL8 secretion from PDAC cells promotes NET formation

The mechanisms underlying NET formation following GnP therapy were investigated. HL-60 cells were induced to neutrophils by ATRA to simulate human neutrophils. MPO-DNA, MPO activity, and SYTOX Green revealed that neutrophils cultured alone did not form NETs when treated with GnP (**Figure 3A–C**). These findings showed that GnP did not directly induce NET formation in neutrophils. However, CM from GnP-resistant cancer cells (MIA PaCa-2 GnP CM and PANC-1 GnP CM) promoted NET formation, which suggested that tumor cells released NET-inducing factors after GnP treatment. A cytokine array was performed on the CM from GnP-sensitive or -resistant MIA PaCa-2 cells to identify candidate factors. The analysis revealed that CXCL8, a neutrophil chemokine, was the most significantly upregulated cytokine in the CM by a volcano plot (**Figure 3D**), a finding corroborated by GO analyses (**Figure 3E**). Importantly, secretion of CXCL8 by GnP-resistant MIA PaCa-2 and PANC-1 cancer cells was confirmed by ELISA (**Figure 3F**). Moreover, neutralizing CXCL8 effectively prevented NET formation induced by CM from GnP-resistant cancer cells (**Figure 3G,H**).

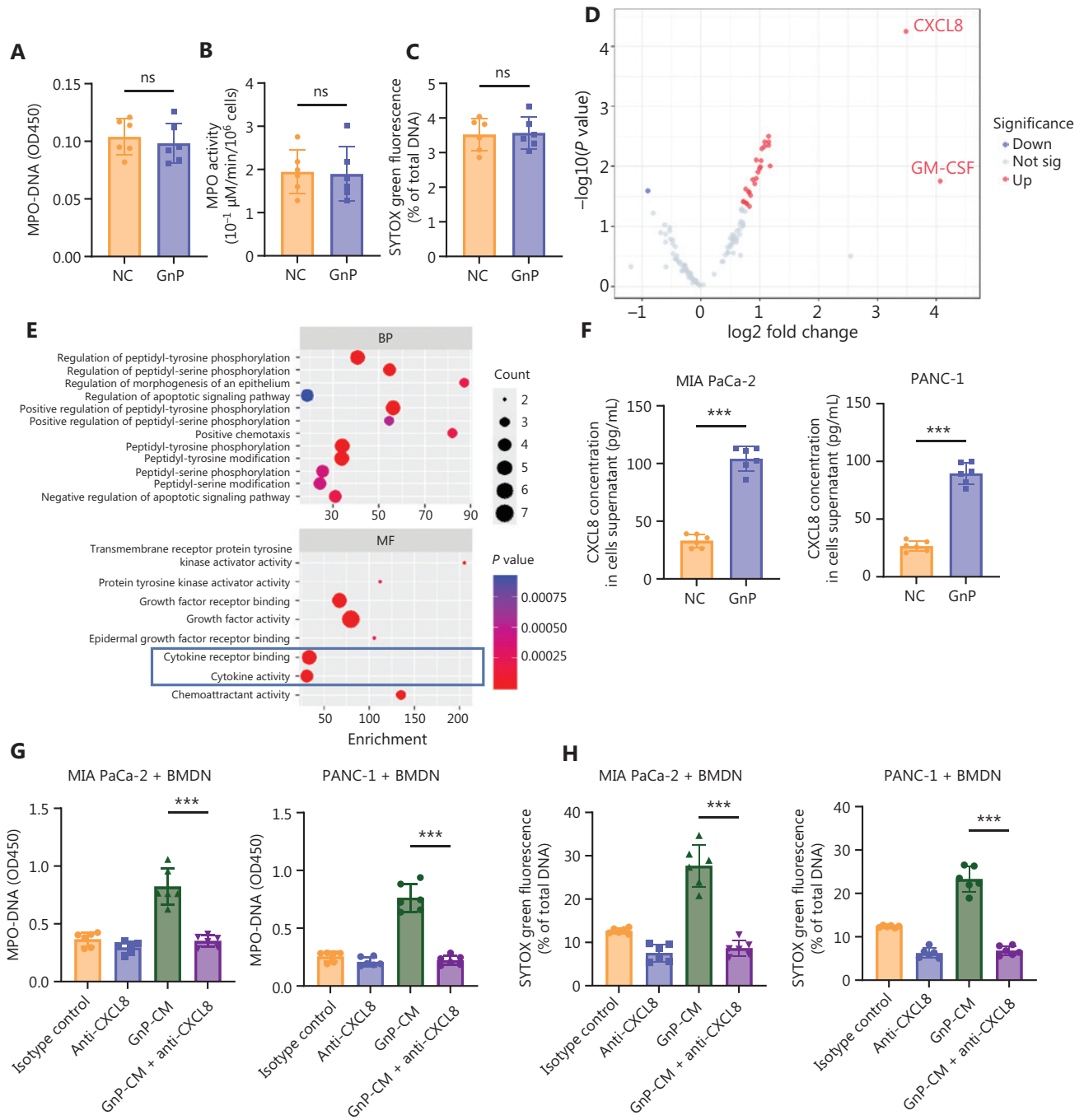


Figure 3 GnP enhances PDAC cells to secrete CXCL8 that promotes NET formation. (A) MPO-DNA, (B) MPO activity, and (C) the fluorescence intensity of SYTOX Green in HL-60-induced neutrophils treated by GnP directly. (D) Volcano plot presenting top two cytokines upregulated by GnP-resistant MIA PaCa-2 culture medium. (E) GO analysis of cytokine array for the supernatant of GnP-sensitive or resistant MIA PaCa-2 cells. (F) Concentration of CXCL8 in the supernatant of GnP-sensitive (NC) or -resistant (GnP) MIA PaCa-2 and PANC-1 cells. (G) MPO-DNA and (H) Fluorescence intensity of SYTOX Green in BMDN treated by media containing isotype control (isotype control), media containing anti-CXCL8 (anti-CXCL8), media from GnP-resistant relative cells (GnP-CM), and GnP-CM + anti-CXCL8. All experiments were performed at least three times. For statistical analyses, an unpaired *t*-test in the case of normal distribution or a non-parametric Mann–Whitney test in the absence of normal distribution was used for (A), (B), (C), and (F). One-way ANOVA was used for (G) and (H). ***, $P < 0.001$; ns, not significant. $n = 6$, Data are the mean ± SD.

GPRC5A-induced CXCL8 secretion promoted NET formation and GnP resistance in PDAC

The mechanisms underlying GnP-induced CXCL8 secretion was investigated. Previous studies have shown that gemcitabine and nab-paclitaxel can affect the levels of HIF1A, cyclin A2[39], GPRC5A[33], CDK2, P21, P27, YAP1, and HO-1 expression[40]. The effect of GnP on these genes was assessed using qRT-PCR and GnP significantly upregulated *GPRC5A*, *HIF1A*, and *YAP1* in MIA PaCa-2 cells (**Figure 4A**). Western blot analysis of these proteins revealed that only GPRC5A expression was notably increased by GnP resistance (**Figure 4B**). GPRC5A knockdown was performed by siRNA in GnP-sensitive or resistant MIA PaCa-2 and PANC-1 cells to determine whether GPRC5A participates in GnP-mediated CXCL8 production (**Figure 4C**). The ELISA results indicated that GPRC5A knockdown reduced CXCL8 secretion in GnP-resistant cells (**Figure 4D**). Similarly, GPRC5A inhibition diminished the ability of GnP-resistant cancer cells to induce NET formation by HL-60-induced neutrophils, as evidenced by MPO-DNA (**Figure 4E**), SYTOX Green (**Figure 4F**), and immunofluorescent staining (**Figure 4G**), and CXCL8 secretion was significantly elevated in GPRC5A-overexpressing GnP-resistant PDAC cells (**Figure S3A**). Moreover, GPRC5A overexpression enhanced NET formation in neutrophils co-cultured with GnP-resistant PDAC cells (**Figure S3B**). Overall, the results suggested that GnP enhanced neutrophil recruitment by inducing GPRC5A-mediated CXCL8 secretion in PDAC cells and CXCL8 promoted NET formation, which ultimately reduced the efficacy of GnP therapy.

GPRC5A regulated CXCL8 expression through nuclear factor kappa B (NF-κB) signaling in GnP-resistant cells

Previous studies have identified several transcription factors, including NF-κB[41], activator protein 1 (AP-1)[42], and activating transcription factor 3 (ATF3)[43], as potential regulators of CXCL8 expression. The levels of these transcription factors were assessed in GnP-resistant PANC-1 cells following GPRC5A knockdown or overexpression to further investigate these findings. NF-κB p65 exhibited expression patterns that correlated with GPRC5A levels (**Figure 5A and 5B**). Notably, NF-κB also showed reduced activation upon GPRC5A knockdown and increased activation upon GPRC5A overexpression, as evidenced by increased cytoplasmic accumulation and decreased nuclear localization of the p65 subunit (**Figure 5C**). Furthermore, treatment with JSH-23, an inhibitor of NF-κB nuclear translocation, significantly reduced both CXCL8 expression and secretion in GnP-resistant PDAC cells (**Figure 5D,E**). These findings collectively supported the conclusion that GPRC5A impairs the therapeutic efficacy of GnP through NF-κB–mediated CXCL8 secretion.

NLRP3 mediates NET formation in PDAC through neutrophil activation

Whether NLRP3 participates in GnP/CXCL8-induced NET formation was further investigated given the critical role of NLRP3 in neutrophil chemotaxis[44] and activation[45]. Neutrophils were exposed to tumor-conditioned medium and an increase in NLRP3 levels in neutrophils was detected by qRT-PCR (**Figure 6A**) and western blot (**Figure 6B**). CXCL8 in the incubation system was inhibited to assess the role of CXCL8 in this process. CXCL8 blocking decreased NLRP3 levels in neutrophils induced by GnP-resistant PDAC cells, as shown by western blot (**Figure 6C**). Consequently, NLRP3 inhibition reduced GnP/CXCL8-induced NET formation, as evidenced by MPO-DNA (**Figure 6D**) and SYTOX Green (**Figure 6E**). NLRP3 inhibition also suppressed LPS-induced MPO-DNA levels (**Figure S4A**) and SYTOX Green intensity, which further supports the role of NLRP3 in NET formation (**Figure S4B**).

GPRC5A inhibition overcomes GnP resistance and improves treatment efficacy in PDAC

Neutrophil-derived DNA is correlated with PDAC patient staging[18]. cfDNA from CM-induced NETs was extracted to further elucidate the role of cfDNA in NET-mediated PDAC cell behavior. The results revealed that cfDNA could promote cell proliferation (**Figure 7A**) and migration (**Figure 7B**). A PDAC model was established by subcutaneously injecting MIA PaCa-2 cells into BALB/c-nude mice, then treating the tumor with PBS (NC), GnP, or GnP + DNase I. The addition of DNase I significantly improved the efficacy of GnP, as evidenced by reduced tumor growth (**Figure 7C**) and prolonged survival (**Figure 7D**). To evaluate the therapeutic potential of targeting GPRC5A in enhancing GnP efficiency, the PDAC model was treated with si-NC, GnP, si-GPRC5A, or GnP + si-GPRC5A. The GnP combined

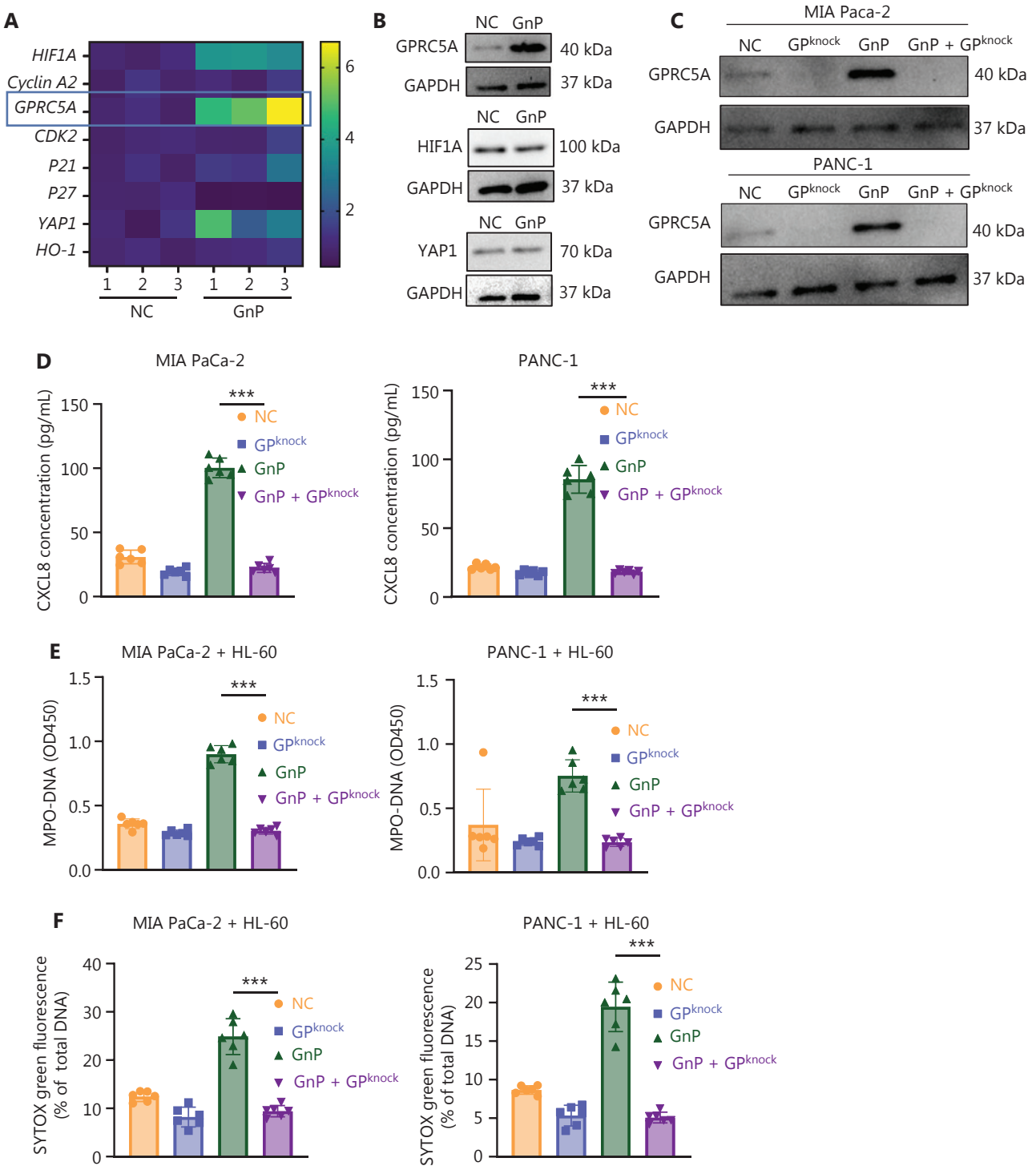


Figure 4 Continued

si-GPRC5A therapy significantly reduced tumor weight (**Figure 7E**) and volume (**Figure 7F**) and inhibited tumor growth (**Figure 7G**). The proportion of neutrophils in $CD45^+$ cells significantly decreased in the GnP + si-GPRC5A group compared to the GnP group, which further supports our hypothesis (**Figure 7H**).

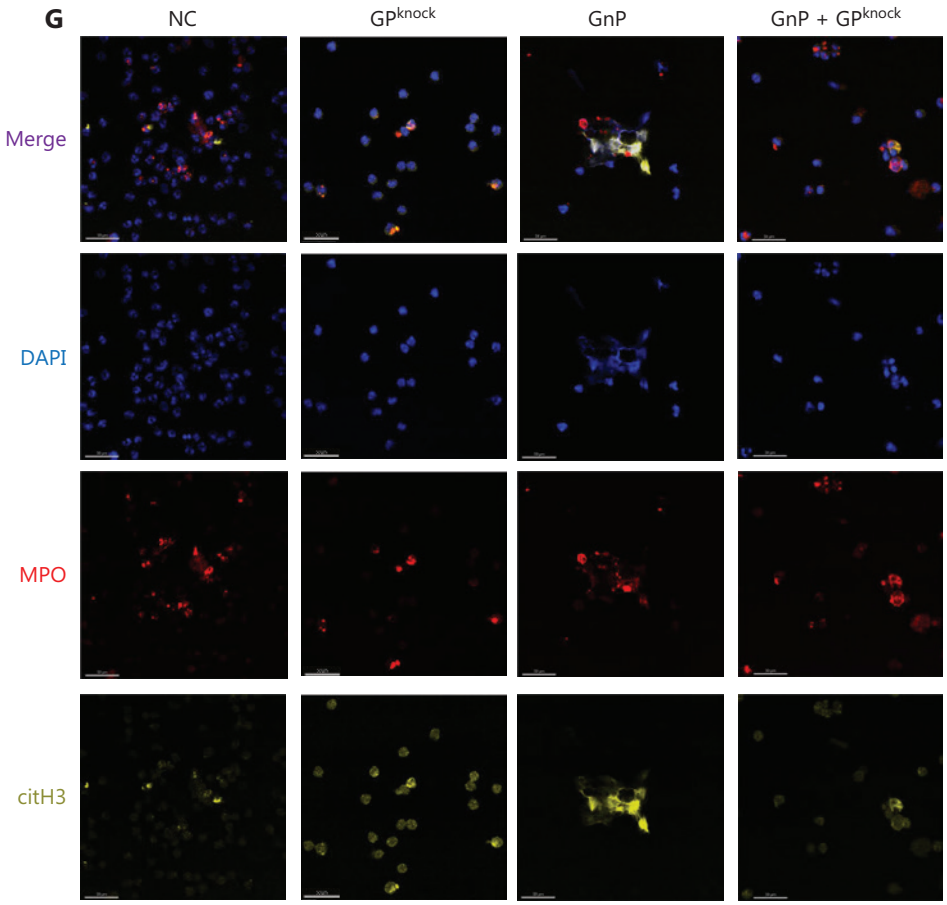


Figure 4 GnP triggers GPRC5A-mediated CXCL8 secretion by PDAC cells and leads to NET formation and chemoresistance. (A) mRNA expression of genes in GnP-sensitive or -resistant MIA PaCa-2 cells, detected by qPCR. (B) HIF1A, GPRC5A, and YAP1 protein expression in GnP-sensitive or -resistant MIA PaCa-2 cells, detected by western blot. (C) GPRC5A protein expression in GnP-sensitive or -resistant MIA PaCa-2 and PANC-1 cells treated by si-NC or si-GPRC5A, detected by western blot. NC: GnP-sensitive PANC-1 cells transfected with si-NC; GP^{knock}: GnP-sensitive PANC-1 cells transfected with si-GPRC5A; GnP: GnP-resistant PANC-1 cells transfected with si-NC; GnP+GP^{knock}: GnP-resistant cells transfected with si-GPRC5A. (D) CXCL8 concentration in the supernatant of GnP-sensitive or -resistant MIA PaCa-2 and PANC-1 cells treated by si-NC or si-GPRC5A, detected by ELISA. (E) MPO-DNA and (F) the fluorescence intensity of SYTOX Green in HL-60-induced neutrophils treated by the supernatant of GnP-sensitive or -resistant MIA PaCa-2 and PANC-1 cells treated by si-NC or si-GPRC5A. (G) Detection of co-localized staining of NETs for DAPI, citrullinated histone H3 (citH3), and myeloperoxidase (MPO) using a confocal microscope in the bone marrow-derived neutrophils treated by the CM of GnP-sensitive or -resistant PANC-1 cells. Scale bar, 50 μm. All experiments were performed at least three times. For statistical analyses, a one-way ANOVA was used for (D), (E), and (F). ***, $P < 0.001$; ns, not significant. $n = 6$, Data are the mean ± SD.

Clinical relevance of GPRC5A expression in PDAC GnP resistance

The *CXCL8*, *GPRC5A*, and *NLRP3* levels between the GnP-responsive and -non-responsive groups were analyzed using data from the TCGA databases. *GPRC5A* and *CXCL8* expression significantly decreased following GnP treatment in the responsive group. Conversely, the non-responsive group displayed elevated *GPRC5A*, *CXCL8*, and *NLRP3* levels after chemotherapy. The GnP-responsive group had lower *NLRP3* levels compared with the non-responsive group before treatment (**Figure 8A**). *CXCL8* levels significantly decreased in neutrophils post-chemotherapy in both groups. However, the reduction in *CXCL8* levels was more pronounced in the responsive group, suggesting a stronger *CXCL8*-suppressive effect of treatment in the responsive

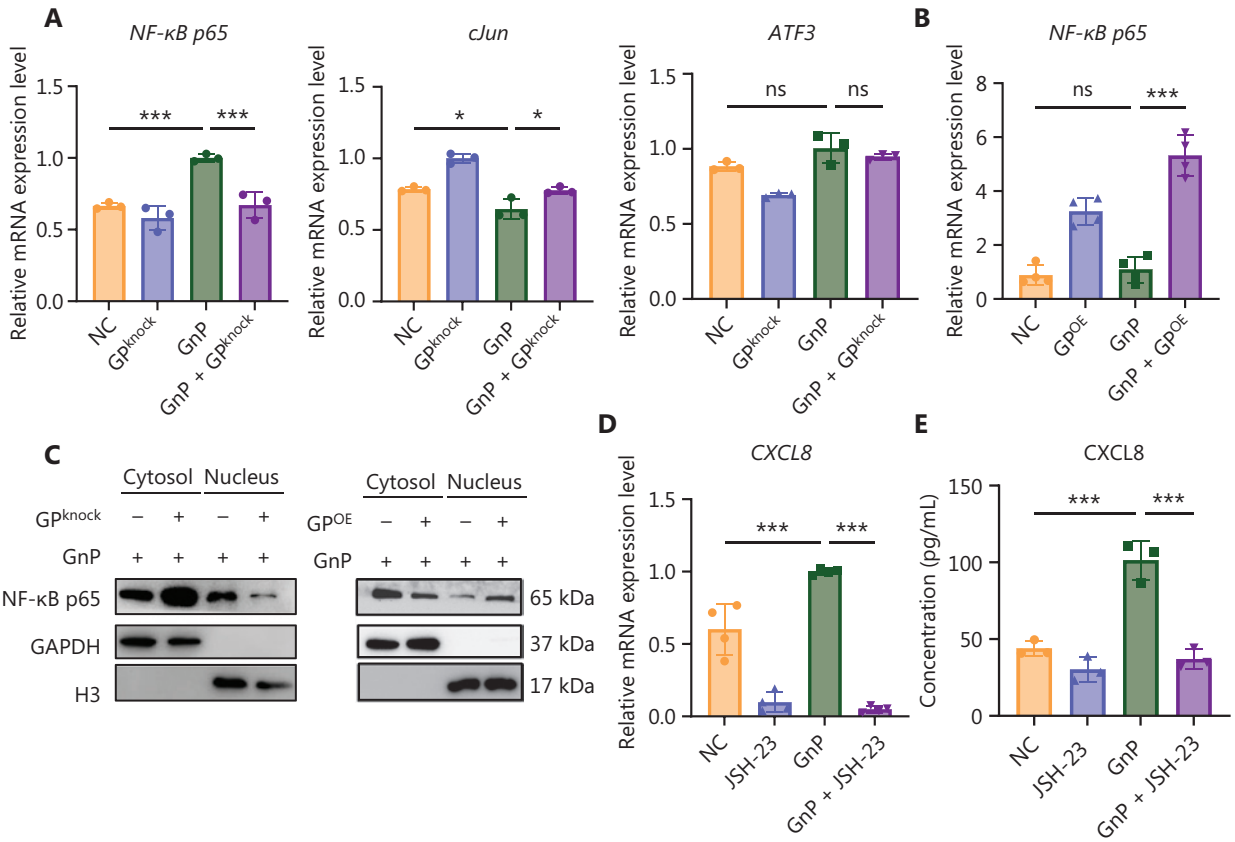


Figure 5 NF-κB activity correlates with GPRC5A expression and modulates CXCL8 secretion. (A) Quantitative PCR analysis of NF-κB p65, cJun, and ATF3 mRNA expression in negative controls (NC), GPRC5A knockdown (GP^{knock}), GnP-resistant (GnP), and GPRC5A knockdown GnP-resistant cells ($GnP+GP^{knock}$). (B) Quantitative PCR analysis of NF-κB p65 mRNA expression in negative controls (NC), GPRC5A overexpressing (GP^{OE}), GnP-resistant (GnP), and GPRC5A overexpressing GnP-resistant cells ($GnP+GP^{OE}$). (C) Western blot analysis of NF-κB p65 in cytoplasm or nuclear of GnP-resistant PANC-1 cells with or without GPRC5A knockdown or overexpression. GP^{OE}: GPRC5A overexpressing PANC-1 cells. (D) Quantitative PCR analysis of CXCL8 mRNA expression in negative controls (NC), JSH-23 (20 μM), GnP-resistant PANC-1 cells (GnP), or JSH-23 treated GnP-resistant PANC-1 cells (GnP + JSH-23). (E) ELISA analysis of CXCL8 levels in the culture supernatants of GnP sensitive or -resistant PANC-1 cells treated with or without JSH-23. For statistical analyses, a one-way ANOVA was used for (A), (B), (D) and (E). Data are presented as the mean ± SD. *, $P < 0.05$; ***, $P < 0.001$; ns, not significant.

group (**Figure 8B**). Tumor samples from patients with PDAC were stained and quantified for GPRC5A by IHC to validate these findings further (**Figure 8C**). The non-responsive group, which was defined as progressive disease after two cycles of GnP treatment, exhibited higher expression of GPRC5A compared to the responsive group, which included complete and partial regression (**Figure 8D**). Elevated GPRC5A expression was associated with a worse PFS in patients with PDAC receiving GnP therapy (**Figure 8E**). Additionally, IF analysis of human PDAC tissues confirmed the co-localization of neutrophils with NLRP3 and CXCL8 (**Figure 8F**).

Discussion

Chemoresistance significantly impaired the effectiveness of GnP therapy and was intricately associated with the complex tumor immune microenvironment in PDAC. GnP therapy mediated NET formation, which in turn promoted chemoresistance in a mouse PDAC model. The findings herein unveiled the release of cfDNA induced by NLRP3 as the key mechanism underlying this chemoresistance and NLRP3 levels were elevated by CXCL8. Cancer cells were the main source of CXCL8 in the current study. GPRC5A was shown to be an essential mediator and cfDNA enhanced tumor cell proliferation and

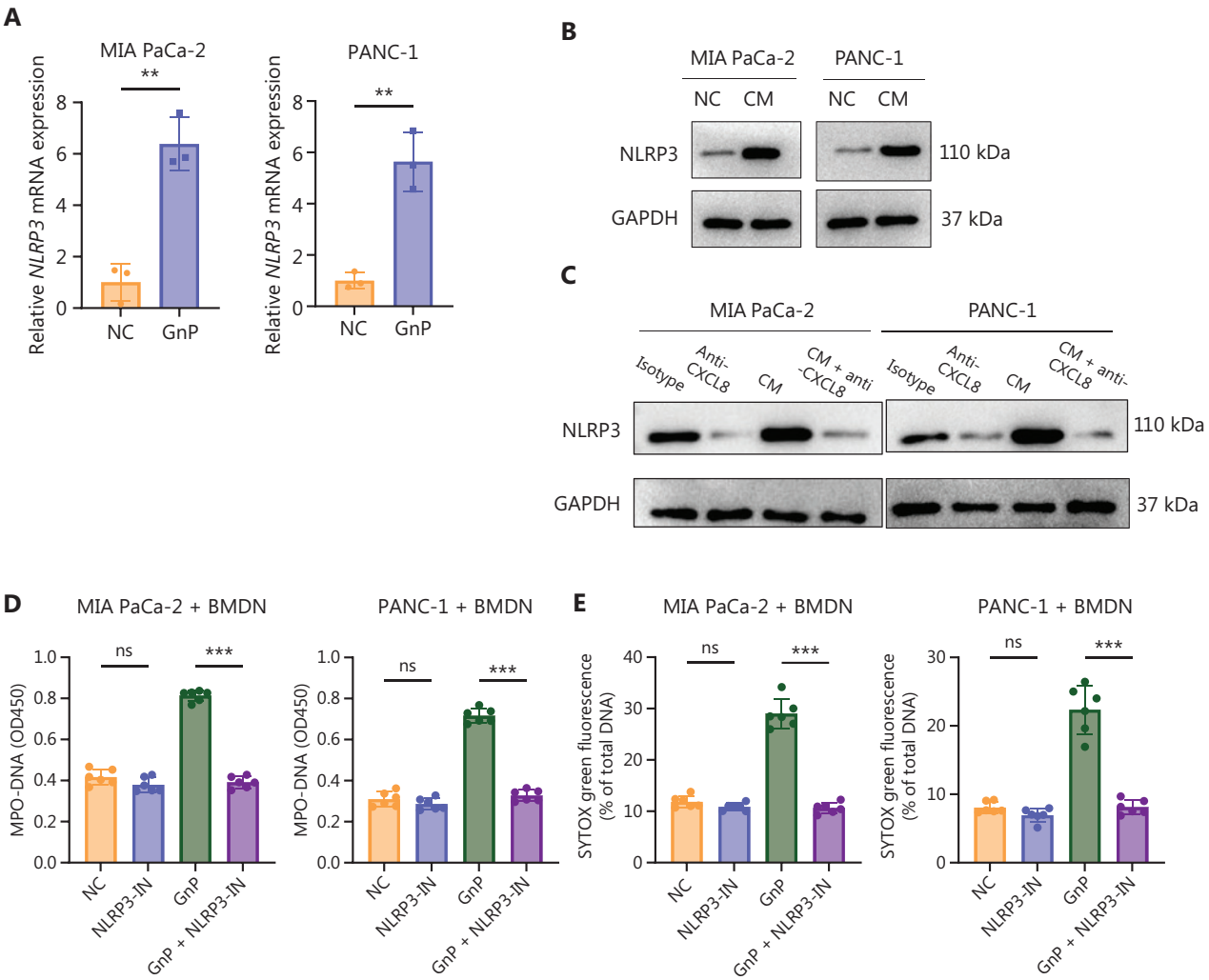


Figure 6 CXCL8 promotes NLRP3 to enhance NET formation (A) mRNA expression and (B) NLRP3 protein expression in BMDNs treated by media or conditional media of GnP-resistant MIA PaCa-2 and PANC-1 cells (CM). (C) NLRP3 protein expression in BMDN treated by media containing isotype control (isotype), media containing anti-CXCL8 (anti-CXCL8), media from GnP-resistant relative cells (GnP-CM), and GnP-CM + anti-CXCL8. (D) MPO-DNA and (E) the fluorescence intensity of SYTOX Green in BMDN treated by the supernatant of GnP-sensitive or -resistant MIA PaCa-2 and PANC-1 cancer cells, and the cancer cells were treated by media (NC) or media + NLRP3-inhibitor (NLRP3 IN). GnP represents the GnP-resistant cancer cells. For statistical analyses, an unpaired *t*-test was used for (A). One-way ANOVA was used for (D) and (E). **, $P < 0.01$; ***, $P < 0.001$; ns, not significant. $n = 6$, Data are the mean ± SD.

migration. The data suggested a role of NETs in GnP resistance in PDAC and this role was improved by targeting the GPRC5A-CXCL8-NET-cfDNA axis.

GnP therapy increased neutrophil chemotaxis into PDAC and induced NET formation within PDAC. Neutrophils are essential infiltrating immunocytes in the PDAC TME[9]. Tumor-infiltrated neutrophils participate in immune suppression, extracellular matrix modification, and tumor progression[46-48]. Clinical studies have shown that tumor-associated neutrophils and NETs are predictive of post-surgical survival in patients with PDAC that is independent of the TNM staging system[49]. In addition, patients exhibiting chemoresistance show a significant increase in plasma NETs after chemotherapy[19]. Cisplatin or adriamycin/cyclophosphamide-treated mouse mammary cancer cells promote NET formation, which reduces the therapeutic effect on lung metastasis of breast cancer[19]. However, a separate study in patients with colorectal cancer reported that chemotherapy-induced NETs inhibit tumor growth[50]. The

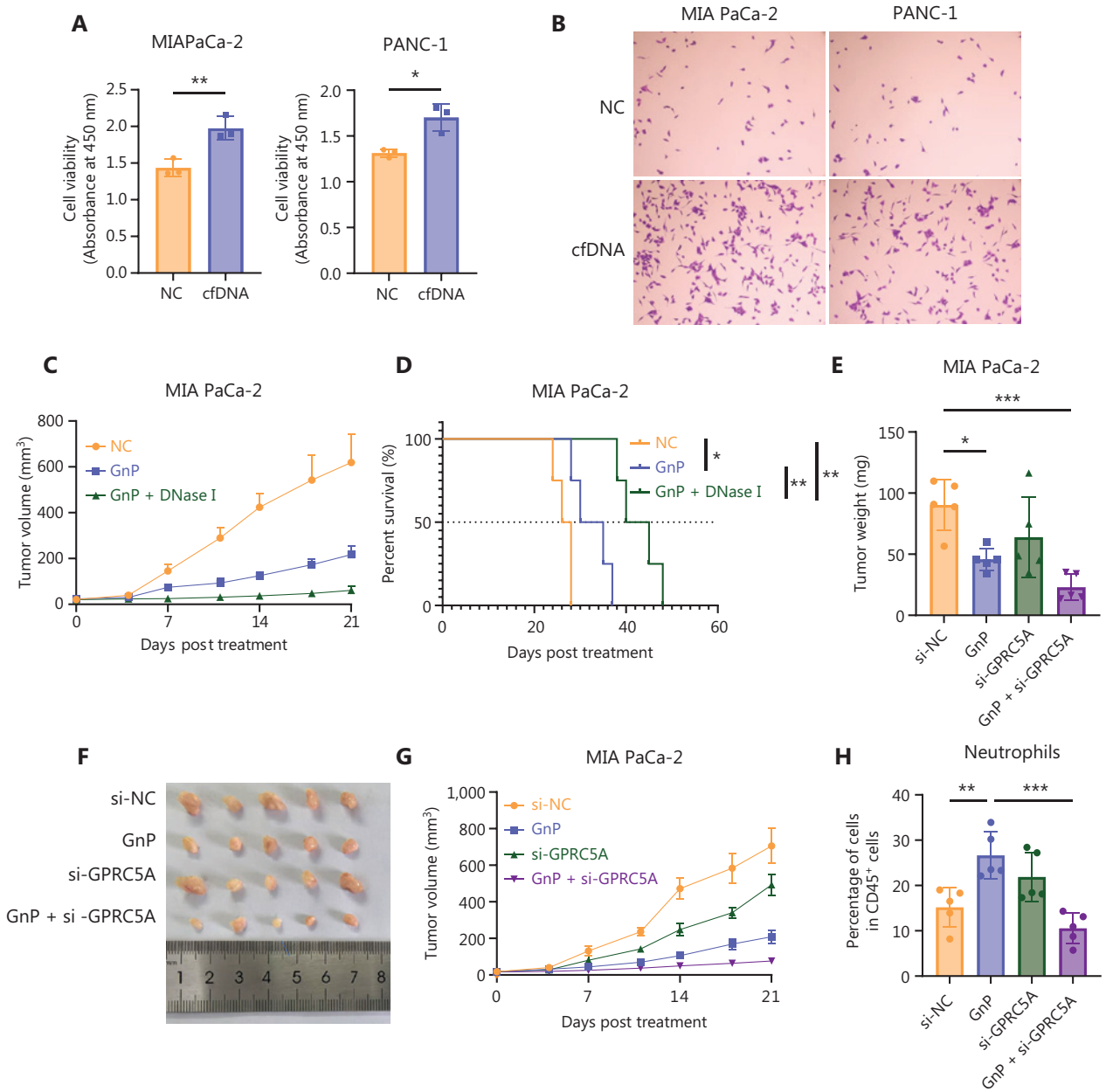


Figure 7 GPRC5A inhibition enhances GnP efficiency in PDAC treatment (A) CCK-8 assay and (B) Transwell cell migration assay of MIA PaCa-2 and PANC-1 cells treated by media (NC) or cell-free DNA (cfDNA). (C) Tumor growth kinetics and (D) survival of MIA PaCa-2 cell bearing BALB/c-nude mice treated with PBS (NC), GnP, or GnP +DNase I (n = 5 per group). (E) Tumor weight, (F) tumor photos, and (G) tumor growth curve of MIA PaCa 2-bearing BALB/c-nude mice that received treatments by si-NC, GnP, si-GPRC5A (GPRC5A knockdown), or GnP + si-GPRC5A when tumor volume reached approximately 20 mm^3. Gemcitabine (100 mg/kg) with albumin-paclitaxel (20 mg/kg) was injected intraperitoneally, si-NC (5 nmol/20 g) or si-GPRC5A (5 nmol/20 g; Ribobio) was injected intratumorally every 4 d for 3 weeks (n = 5 per group). (H) The proportion of neutrophils in the total $CD45^+$ cell sample in tumor tissues of si-NC, GnP, si-GRPC5A, or GnP + si-GPRC5A-treated MIA PaCa-2-bearing BALB/c-nude mice. All experiments were performed at least three times. For statistical analyses, an unpaired t-test was used for (A). The P value shown in (D), (F), and (H) was determined by one-way ANOVA. *, $P < 0.05$; **, $P < 0.01$; ***, $P < 0.001$; ns, not significant. Data are the mean ± SD.

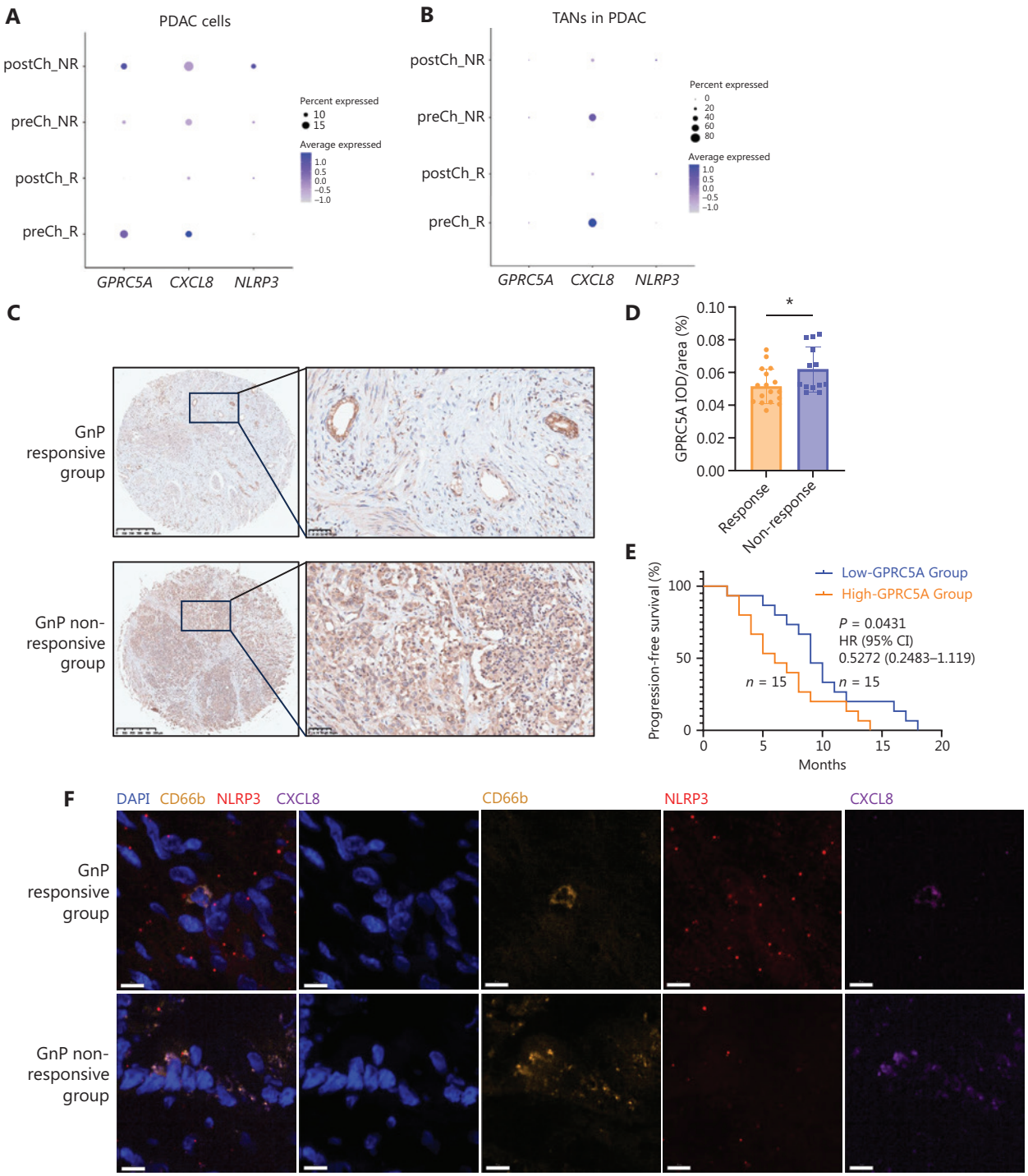


Figure 8 GPRC5A correlated with GnP efficiency in patients with PDAC (A) GPRC5A, CXCL8, and NLRP3 expression in PDAC cells and (B) Tumor-associated neutrophils (TANs) before and after GnP treatment and between responsive and non-responsive groups among patients with PDAC. postCh_NR: post chemotherapy non-responsive group; preCh_NR: pre-chemotherapy non-responsive group; postCh_R: post-chemotherapy responsive group; preCh_R: pre-chemotherapy responsive group. (C) Representative immunohistochemistry of pancreatic tumor (n = 30) stained with GPRC5A for the GnP-responsive and -non-responsive groups, respectively. Scale bar, 500 μm (left), 50 μm (right). (D) Quantification of the IHC staining (n = 30) The responsive group included patients with complete and partial responses (n = 17). The non-responsive group includes patients with progressive disease (n = 13). The GPRC5A expression was calculated by integrated density/

area. (E) Survival analysis between GPRC5A staining intensity and PFS of patients with pancreatic cancer after GnP treatment and the cut-off value was the median of the GPRC5A IOD/area. The median PFS of the low and high GPRC5A groups were 9 and 6 months, respectively. (F) Representative immunofluorescence of pancreatic tumor (n = 30) for co-localization of CD66b (yellow), NLRP3 (red), and CXCL8 (purple). Scale bar, 10 μm. The P value shown was determined by Student's t-test (D) and the log-rank test in (E). *, $P < 0.05$; Data are the mean ± SD.

divergent findings in the current study may be attributed to differences in cancer types and stages.

NETs were undetectable in normal tissues in the current study but were present in the blood of tumor-bearing mice, which suggested that GnP-induced NETs were tumor-dependent. Whether GnP modulates NETs in PDAC cells was investigated given that GnP primarily targets tumor cells; *in vitro* experiments confirmed that hypothesis. NETs facilitate PDAC cell migration[51]. PAD4 knockout significantly reduces NET formation, cfDNA, and tumor growth in a pancreatic cancer mouse model, which aligned with the findings herein that NETs contribute to PDAC tumor cell proliferation and migration[18]. The reciprocal promotion between NETs and tumor cells led to resistance to GnP therapy. Therefore, NET inhibition may disturb this feedback loop and enhance GnP efficiency.

The current study findings confirmed, for the first time, that GnP can promote the secretion of CXCL8 by GPRC5A expression of PDAC cells. GnP-treated neutrophils did not produce NETs, which indicated that GnP induced NET production through PDAC cells. Cytokine array analysis revealed that CXCL8 was the most significantly upregulated cytokine in the CM of GnP-resistant MIA PaCa-2 cells. This finding was supported by other studies that showed gemcitabine increases CXCL8 levels in pancreatic cancer cells[52]. In agreement with the current study findings, CXCL8 recruits neutrophils and induces NET formation[53-55]. The density of NETs in the TME of patients with non-small cell lung cancer (NSCLC), bladder cancer, and metastatic melanoma is positively correlated with CXCL8 protein expression and the density of NETs in peripheral blood of patients with melanoma and NSCLC is positively correlated with CXCL8[56]. Blocking CXCL8 did not improve the chemotherapy efficacy of MIA PaCa-2 cells when using NET CM to treat PDAC cells. This finding provided support that CXCL8, which induces NET formation, is from PDAC cells. In another study, NETs capture colorectal cancer cells in the liver, which promotes CXCL8 production and induces NET formation; this positive feedback promotes liver metastasis in colorectal cancer[57].

The mechanisms underlying GnP-induced CXCL8 secretion by PDAC cells was explored and GPRC5A was shown to have a key role. Inhibition of GPRC5A significantly reduced GnP-induced NET formation, although GPRC5A itself does not directly influence the effects of NETs on tumor cells. Inhibition of GPRC5A hampers the nuclear translocation of NF-κB, which accounts for the decrease in CXCL8 secretion in GnP-resistant PDAC cells. GPRC5A not only participates in the occurrence and progression of PDAC[32] but also contributes to chemotherapy resistance[33,34]. Gemcitabine-induced stress in PDAC cells elevates GPRC5A protein levels[34].

The current study also revealed that cfDNA produced by NETs promoted the proliferation and migration of PDAC cells. Targeting cfDNA can improve the effectiveness of GnP therapy. cfDNA refers to highly fragmented DNA released by various cell types and neutrophils produce much more cfDNA than PDAC cells. This finding is consistent with other reports that cfDNA is mainly from neutrophils in pancreatic cancer patients[58]. Circulating neutrophil-derived DNA correlates with staging in patients with PDAC[18]. cfDNA also presents a similar effect in promoting the proliferation and migration of tumor cells in breast and liver cancers[59,60]. Therefore, the combination of GnP and DNase can significantly improve the effectiveness of GnP.

The current study also demonstrated that targeting GPRC5A and cfDNA holds therapeutic potential for overcoming GnP resistance. Application of si-GPRC5A in conjunction with GnP therapy significantly reduced tumor growth and decreased the proportion of neutrophils within the tumor. Moreover, combining DNase with GnP therapy enhanced survival in tumor-bearing mice. These findings indicated that GPRC5A and cfDNA contributed to resistance against GnP therapy, highlighting the potential for clinical application. Therefore, further research using patient-derived xenograft (PDX) models or biomaterial-based delivery systems is needed to validate this mechanism by effectively targeting GPRC5A inhibition.

Although the current study focused on neutrophil-mediated mechanisms, the tumor immune microenvironment in PDAC is highly complex. Specifically, tumor-associated macrophages (TAMs) have been implicated in promoting gemcitabine through the macrophage-CCL5-Sp1-AGEG feedback loop

between macrophages and pancreatic cancer cells[61]. Therefore, future investigations incorporating multiple immune cell types, including macrophages, may provide a more comprehensive understanding of resistance mechanisms to GnP.

This study had several limitations. First, syngeneic mouse models were not utilized because mice lack a homolog for human CXCL8. However, CXCR1 and CXCR2 expression could be analyzed in mice as an alternative. Given the heterogeneity of first-line chemotherapy regimens in pancreatic cancer, along with the limited availability of surgical specimens and complete follow-up data, the sample size in this study was relatively constrained. Further validation in larger, independent cohorts is warranted to confirm the role of GPRC5A in GnP resistance. Finally, although this study demonstrated that GnP therapy enhanced CXCL8 secretion, whether this effect was specific to GnP therapy or a common feature of other standard chemotherapeutic drugs remains unclear.

Conclusions

In summary, the findings herein demonstrated increased CXCL8 secretion by PDAC cells through GPRC5A upregulation. Therefore, CXCL8 triggers NLRP3-mediated NET formation and NET-derived cfDNA contributes to chemoresistance by promoting tumor cell proliferation and motility. GnP combination therapy and cfDNA clearance or GPRC5A inhibition was significantly more efficient than respective monotherapy (**Figure 9**). These findings may lead to new therapeutic strategies *via* targeting the GPRC5A-CXCL8-NET-cfDNA axis to

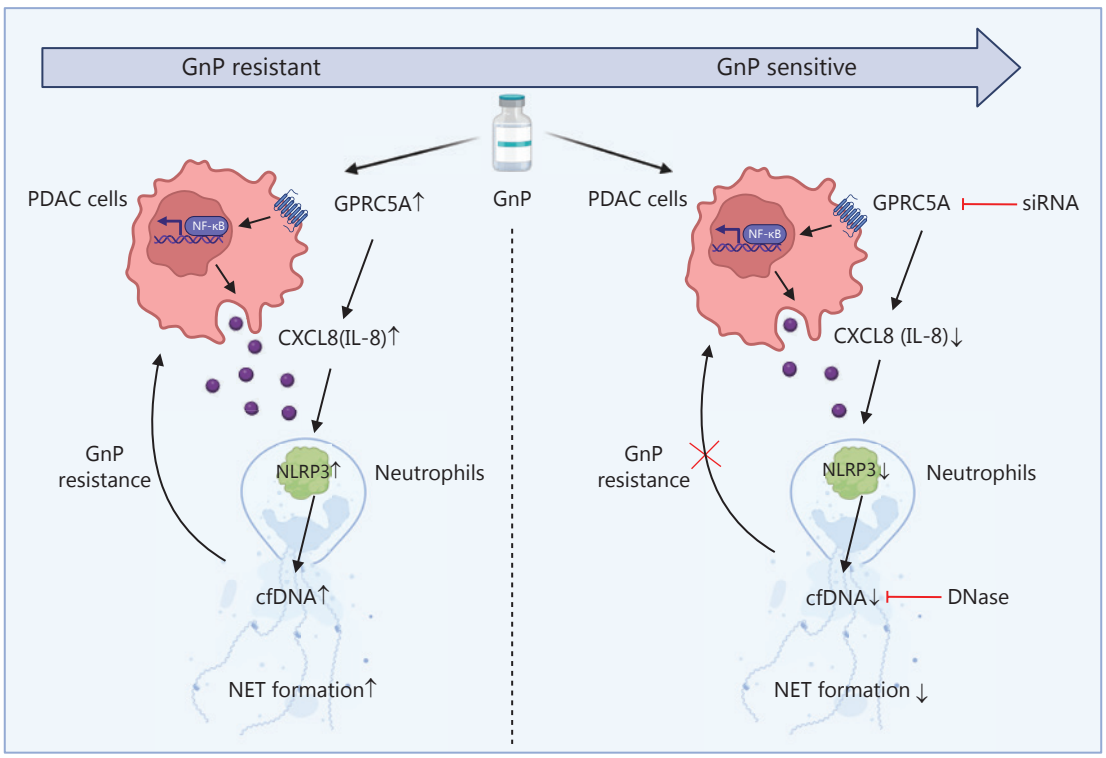


Figure 9 Schematic illustration of the mechanism underlying GPRC5A in GnP resistance. This schematic illustrates the mechanism underlying gemcitabine and nab-paclitaxel (GnP) resistance in pancreatic ductal adenocarcinoma (PDAC) and how inhibition of this pathway restored sensitivity. In the GnP-resistant context, PDAC cells exhibit upregulated GPRC5A expression, which activated NF-κB signaling. This led to elevated transcription and secretion of the chemokine, CXCL8 (also known as IL-8). CXCL8 recruited neutrophils and promoted activation of the NLRP3 within neutrophils, resulting in the release of cell-free DNA (cfDNA). cfDNA, in turn, contributed to the development and maintenance of resistance to gemcitabine and nab-paclitaxel (GnP) in PDAC cells through a feedback loop. In contrast, inhibition of GPRC5A by siRNA suppressed NF-κB-mediated CXCL8 secretion, reduced neutrophil recruitment and NLRP3 activation, and limited cfDNA release. This disruption of the GPRC5A–CXCL8–NLRP3 signaling cascade attenuated the tumor-promoting microenvironment and restored GnP sensitivity. Direct degradation of cfDNA using DNase similarly enhanced the sensitivity of PDAC cells to GnP treatment. Red bars indicate inhibitory events, while arrows represent activation or promotion (created with Biorender.com).

overcome chemoresistance and improve treatment outcomes for patients with PDAC.

Grant support

This work was supported by the National Natural Science Foundation of China (Grant Nos. 82271883 and 82073195 to Qing.Xia; and 82471775 and 82271800 to Yuli.Lin), the Hospital-pharma Integration Project on Innovative Achievement Translation (Grant No. SHDC2022CRD043 to Qing.Xia), the Shanghai Jiao Tong University School of Medicine Summit Program – "Research Physician" in Clinical Medicine to Qing.Xia, the Young Physician-Scientist Cultivation Program of Shanghai Immune Therapy Institute to Qing.Xia, and the Light of the Lintel-young Talents of Huangpu to Qing.Xia.

Conflict of interest statement

No potential conflicts of interest are disclosed.

Author contributions

Conceived and designed the analysis: Tianyi Zhu, Jian Gao, Yuli Lin, Qing Xia.
Collected the data: Tianyi Zhu, Qianwen Yang, Jian Gao.
Contributed data or analysis tools: Xiaozhe Qian, Jianchen Fang, Xiuqi Wu, Yukuan Feng, Jian Gao.
Performed the analysis: Tianyi Zhu, Qianwen Yang, Xiaozhe Qian, Xiuqi Wu, Jian Gao.
Wrote the paper: Tianyi Zhu, Jian Gao, Yuli Lin, Qing Xia.

References

1. Hu ZI, O'Reilly EM. Therapeutic developments in pancreatic cancer. Nat Rev Gastroenterol Hepatol. 2024; 21: 7-24.
2. Hilmi M, Delaye M, Muzzolini M, Nicolle R, Cros J, Hammel P, et al. The immunological landscape in pancreatic ductal adenocarcinoma and overcoming resistance to immunotherapy. Lancet Gastroenterol Hepatol. 2023; 8: 1129-42.
3. Siegel RL, Giaquinto AN, Jemal A. Cancer statistics, 2024. CA Cancer J Clin. 2024; 74: 12-49.
4. Tempero MA, Pelzer U, O'Reilly EM, Winter J, Oh DY, Li CP, et al. Adjuvant *nab*-paclitaxel + gemcitabine in resected pancreatic ductal adenocarcinoma: results from a randomized, open-label, phase III trial. J Clin Oncol. 2023; 41: 2007-19.
5. Von Hoff DD, Ervin T, Arena FP, Chiorean EG, Infante J, Moore M, et al. Increased survival in pancreatic cancer with nab-paclitaxel plus gemcitabine. N Engl J Med. 2013; 369: 1691-703.
6. Tempero MA, Malafa MP, Al-Hawary M, Behrman SW, Benson AB, Cardin DB, et al. Pancreatic adenocarcinoma, version 2.2021, NCCN Clinical Practice Guidelines in Oncology. J Natl Compr Canc Netw. 2021; 19: 439-57.
7. Natu J, Nagaraju GP. Gemcitabine effects on tumor microenvironment of pancreatic ductal adenocarcinoma: special focus on resistance mechanisms and metronomic therapies. Cancer Lett. 2023; 573: 216382.
8. Mahajan UM, Langhoff E, Goni E, Costello E, Greenhalf W, Halloran C, et al. Immune cell and stromal signature associated with progression-free survival of patients with resected pancreatic ductal adenocarcinoma. Gastroenterology. 2018; 155: 1625-39.
9. Jin L, Kim HS, Shi J. Neutrophil in the pancreatic tumor microenvironment. Biomolecules. 2021; 11: 1170.
10. Fridlender ZG, Sun J, Kim S, Kapoor V, Cheng G, Ling L, et al. Polarization of tumor-associated neutrophil phenotype by TGF-beta: "N1" versus "N2" TAN. Cancer Cell. 2009; 16: 183-94.
11. Wang L, Liu Y, Dai Y, Tang X, Yin T, Wang C, et al. Single-cell RNA-seq analysis reveals BHLHE40-driven pro-tumour neutrophils with hyperactivated glycolysis in pancreatic tumour microenvironment. Gut. 2022; 72: 958-71.
12. Zhang S, Fang W, Zhou S, Zhu D, Chen R, Gao X, et al. Single cell transcriptomic analyses implicate an immunosuppressive tumor microenvironment in pancreatic cancer liver metastasis. Nat Commun. 2023; 14: 5123.
13. Adrover JM, McDowell SAC, He XY, Quail DF, Egeblad M. NETworking with cancer: the bidirectional interplay between cancer and neutrophil extracellular traps. Cancer Cell. 2023; 41: 505-26.
14. Chen X, Ma H, Mo S, Yu S, Lu Z, Chen J. Intratumoral neutrophil extracellular traps are associated with unfavorable clinical outcomes and immunogenic context in pancreatic ductal adenocarcinoma. Front Immunol. 2022; 13: 1027459.
15. Hackner D, Merkel S, Weiß A, Krautz C, Weber GF, Grützmann R, et al. Neutrophil-to-lymphocyte ratio and prognostic nutritional index are predictors for overall survival after primary pancreatic resection of pancreatic ductal adenocarcinoma: a single centre evaluation. Cancers (Basel). 2024; 16: 2911.
16. Varzaru B, Iacob RA, Bunduc S, Manea I, Sorop A, Spiridon A, et al. Prognostic value of circulating cell-free DNA concentration and neutrophil-to-lymphocyte ratio in patients with pancreatic ductal adenocarcinoma: a prospective cohort study. Int J Mol Sci. 2024; 25: 2854.
17. Cristinziano L, Modestino L, Antonelli A, Marone G, Simon HU, Varricchi G, et al. Neutrophil extracellular traps in cancer. Semin Cancer Biol. 2022; 79: 91-104.
18. Miller-Ocuin JL, Liang X, Boone BA, Doerfler WR, Singhi AD, Tang D, et al. DNA released from neutrophil extracellular traps (NETs) activates pancreatic stellate cells and enhances pancreatic tumor growth. Oncoimmunology. 2019; 8: e1605822.

19. Mousset A, Lecorgne E, Bourget I, Lopez P, Jenovai K, Cherfils-Vicini J, et al. Neutrophil extracellular traps formed during chemotherapy confer treatment resistance via TGF-β activation. Cancer Cell. 2023; 41: 757-75.
20. Idorn M, Skadborg SK, Kellermann L, Halldorsdottir HR, Holmen Olofsson G, Met O, et al. Chemokine receptor engineering of T cells with CXCR2 improves homing towards subcutaneous human melanomas in xenograft mouse model. Oncoimmunology. 2018; 7: e1450715.
21. Shang A, Gu C, Zhou C, Yang Y, Chen C, Zeng B, et al. Exosomal KRAS mutation promotes the formation of tumor-associated neutrophil extracellular traps and causes deterioration of colorectal cancer by inducing IL-8 expression. Cell Commun Signal. 2020; 18: 52.
22. Schoeps B, Eckfeld C, Prokopchuk O, Böttcher J, Häußler D, Steiger K, et al. TIMP1 triggers neutrophil extracellular trap formation in pancreatic cancer. Cancer Res. 2021; 81: 3568-79.
23. Zhang Y, Chandra V, Riquelme Sanchez E, Dutta P, Quesada PR, Rakoski A, et al. Interleukin-17-induced neutrophil extracellular traps mediate resistance to checkpoint blockade in pancreatic cancer. J Exp Med. 2020; 217: e20190354.
24. Bun M, Kawano M, Yamamoto G, Sakata M, Shimura K, Toda A, et al. G-CSF induces neutrophil extracellular traps formation and promotes ovarian cancer peritoneal dissemination. J Leukoc Biol. 2024; 116: 1157-68.
25. Murthy P, Zenati MS, AlMasri SS, DeSilva A, Singhi AD, Paniccia A, et al. Impact of recombinant granulocyte colony-stimulating factor during neoadjuvant therapy on outcomes of resected pancreatic cancer. J Natl Compr Canc Netw. 2023; 22: e237070.
26. Jablonska E, Garley M, Surazynski A, Grubczak K, Iwaniuk A, Borys J, et al. Neutrophil extracellular traps (NETs) formation induced by TGF-β in oral lichen planus – possible implications for the development of oral cancer. Immunobiology. 2020; 225: 151901.
27. Jin R, Xu J, Gao Q, Mao X, Yin J, Lu K, et al. IL-33-induced neutrophil extracellular traps degrade fibronectin in a murine model of bronchopulmonary dysplasia. Cell Death Discov. 2020; 6: 33.
28. Park J, Wysocki RW, Amoozgar Z, Maiorino L, Fein MR, Jorns J, et al. Cancer cells induce metastasis-supporting neutrophil extracellular DNA traps. Sci Transl Med. 2016; 8: 361ra138.
29. Wang CY, Lin TT, Hu L, Xu CJ, Hu F, Wan L, et al. Neutrophil extracellular traps as a unique target in the treatment of chemotherapy-induced peripheral neuropathy. EBioMedicine. 2023; 90: 104499.
30. Tao Q, Fujimoto J, Men T, Ye X, Deng J, Lacroix L, et al. Identification of the retinoic acid-inducible Gprc5a as a new lung tumor suppressor gene. J Natl Cancer Inst. 2007; 99: 1668-82.
31. Liu S, Ye D, Wang T, Guo W, Song H, Liao Y, et al. Repression of GPRC5A is associated with activated STAT3, which contributes to tumor progression of head and neck squamous cell carcinoma. Cancer Cell Int. 2017; 17: 34.
32. Liu D, Jin Y, Wu J, Zhu H, Ye D. MiR-135b-5p is an oncogene in pancreatic cancer to regulate GPRC5A expression by targeting transcription factor KLF4. Cell Death Discov. 2022; 8: 23.
33. Zhou H, Telonis AG, Jing Y, Xia NL, Biederman L, Jimbo M, et al. GPRC5A is a potential oncogene in pancreatic ductal adenocarcinoma cells that is upregulated by gemcitabine with help from HuR. Cell Death Dis. 2016; 7: e2294.
34. Liu B, Yang H, Pilarsky C, Weber GF. The effect of GPRC5a on the proliferation, migration ability, chemotherapy resistance, and phosphorylation of GSK-3β in pancreatic cancer. Int J Mol Sci. 2018; 19: 1870.
35. Hayden H, Ibrahim N, Klopf J, Zagrapan B, Mauracher LM, Hell L, et al. ELISA detection of MPO-DNA complexes in human plasma is error-prone and yields limited information on neutrophil extracellular traps formed in vivo. PLoS One. 2021; 16: e0250265.
36. Jiang SH, Zhu LL, Zhang M, Li RK, Yang Q, Yan JY, et al. GABRP regulates chemokine signalling, macrophage recruitment and tumour progression in pancreatic cancer through tuning KCNN4-mediated Ca^{2+} signalling in a GABA-independent manner. Gut. 2019; 68: 1994-2006.
37. Du P, Ma Q, Zhu ZD, Li G, Wang Y, Li QQ, et al. Mechanism of Corilagin interference with IL-13/STAT6 signaling pathways in hepatic alternative activation macrophages in schistosomiasis-induced liver fibrosis in mouse model. Eur J Pharmacol. 2016; 793: 119-26.
38. Suzuki R, Takagi T, Hikichi T, Konno N, Sugimoto M, Watanabe KO, et al. Derived neutrophil/lymphocyte ratio predicts gemcitabine therapy outcome in unresectable pancreatic cancer. Oncol Lett. 2016; 11: 3441-45.
39. Chen YH, Chen YC, Lin CC, Hsieh YP, Hsu CS, Hsieh MC. Synergistic anticancer effects of gemcitabine with pitavastatin on pancreatic cancer cell line MIA PaCa-2 in vitro and in vivo. Cancer Manag Res. 2020; 12: 4645-65.
40. Ahmad IM, Dafferner AJ, O'Connell KA, Mehla K, Britigan BE, Hollingsworth MA, et al. Heme oxygenase-1 inhibition potentiates the effects of nab-paclitaxel-gemcitabine and modulates the tumor microenvironment in pancreatic ductal adenocarcinoma. Cancers (Basel). 2021; 13: 2264.
41. Zhai J, Shen J, Xie G, Wu J, He M, Gao L, et al. Cancer-associated fibroblasts-derived IL-8 mediates resistance to cisplatin in human gastric cancer. Cancer Lett. 2019; 454: 37-43.
42. Lian S, Li S, Zhu J, Xia Y, Do Jung Y. Nicotine stimulates IL-8 expression via ROS/NF-κB and ROS/MAPK/AP-1 axis in human gastric cancer cells. Toxicology. 2022; 466: 153062.
43. Palombo R, Passacantilli I, Terracciano F, Capone A, Matteocci A, Tournier S, et al. Inhibition of the PI3K/AKT/mTOR signaling promotes an M1 macrophage switch by repressing the ATF3-CXCL8 axis in Ewing sarcoma. Cancer Lett. 2023; 555: 216042.
44. Van Bruggen S, Jarrot PA, Thomas E, Sheehy CE, Silva CMS, Hsu AY, et al. NLRP3 is essential for neutrophil polarization and chemotaxis in response to leukotriene B4 gradient. Proc Natl Acad Sci U S A. 2023; 120: e2303814120.
45. Pruenster M, Immler R, Roth J, Kuchler T, Bromberger T, Napoli M, et al. E-selectin-mediated rapid NLRP3 inflammasome activation regulates S100A8/S100A9 release from neutrophils via transient gasdermin D pore formation. Nat Immunol. 2023; 24: 2021-31.

46. Xiong S, Dong L, Cheng L. Neutrophils in cancer carcinogenesis and metastasis. J Hematol Oncol. 2021; 14: 173.
47. Hedrick CC, Malanchi I. Neutrophils in cancer: heterogeneous and multifaceted. Nat Rev Immunol. 2022; 22: 173-87.
48. Que H, Fu Q, Lan T, Tian X, Wei X. Tumor-associated neutrophils and neutrophil-targeted cancer therapies. Biochim Biophys Acta Rev Cancer. 2022; 1877: 188762.
49. Jin W, Xu HX, Zhang SR, Li H, Wang WQ, Gao HL, et al. Tumor-infiltrating NETs predict postsurgical survival in patients with pancreatic ductal adenocarcinoma. Ann Surg Oncol. 2019; 26: 635-43.
50. Li Y, Wu S, Zhao Y, Dinh T, Jiang D, Selfridge JE, et al. Neutrophil extracellular traps induced by chemotherapy inhibit tumor growth in murine models of colorectal cancer. J Clin Invest. 2024; 134: e175031.
51. Jin W, Yin H, Li H, Yu XJ, Xu HX, Liu L. Neutrophil extracellular DNA traps promote pancreatic cancer cells migration and invasion by activating EGFR/ERK pathway. J Cell Mol Med. 2021; 25: 5443-56.
52. Deshmukh SK, Tyagi N, Khan MA, Srivastava SK, Al-Ghadhban A, Dugger K, et al. Gemcitabine treatment promotes immunosuppressive microenvironment in pancreatic tumors by supporting the infiltration, growth, and polarization of macrophages. Sci Rep. 2018; 8: 12000.
53. Su X, Brassard A, Bartolomucci A, Dhoparee-Doomah I, Qiu Q, Tsering T, et al. Tumour extracellular vesicles induce neutrophil extracellular traps to promote lymph node metastasis. J Extracell Vesicles. 2023; 12: e12341.
54. Peng ZP, Jiang ZZ, Guo HF, Zhou MM, Huang YF, Ning WR, et al. Glycolytic activation of monocytes regulates the accumulation and function of neutrophils in human hepatocellular carcinoma. J Hepatol. 2020; 73: 906-17.
55. Dhayni K, Zibara K, Issa H, Kamel S, Bennis Y. Targeting CXCR1 and CXCR2 receptors in cardiovascular diseases. Pharmacol Ther. 2022; 237: 108257.
56. de Andrea CE, Ochoa MC, Villalba-Esparza M, Teijeira A, Schalper KA, Abengozar-Muela M, et al. Heterogenous presence of neutrophil extracellular traps in human solid tumours is partially dependent on IL-8. J Pathol. 2021; 255: 190-201.
57. Yang L, Liu L, Zhang R, Hong J, Wang Y, Wang J, et al. IL-8 mediates a positive loop connecting increased neutrophil extracellular traps (NETs) and colorectal cancer liver metastasis. J Cancer. 2020; 11: 4384-96.
58. Mattox AK, Douville C, Wang Y, Popoli M, Ptak J, Silliman N, et al. The origin of highly elevated cell-free DNA in healthy individuals and patients with pancreatic, colorectal, lung, or ovarian cancer. Cancer Discov. 2023; 13: 2166-79.
59. Yang L, Liu Q, Zhang X, Liu X, Zhou B, Chen J, et al. DNA of neutrophil extracellular traps promotes cancer metastasis via CCDC25. Nature. 2020; 583: 133-38.
60. Dickson I. NETs promote liver metastasis via CCDC25. Nat Rev Gastroenterol Hepatol. 2020; 17: 451.
61. Jiang S, Deng T, Cheng H, Liu W, Shi D, Yuan J, et al. Macrophage-organoid co-culture model for identifying treatment strategies against macrophage-related gemcitabine resistance. J Exp Clin Cancer Res. 2023; 42: 199.

Cite this article as: Zhu T, Yang Q, Qian X, Wu X, Fang J, Lin Y, et al. GPRC5A/CXCL8/NLRP3-mediated neutrophil extracellular traps drive gemcitabine-nab-paclitaxel resistance in pancreatic adenocarcinoma. Cancer Biol Med. 2025; 22: 832-853. doi: 10.20892/j.issn.2095-3941.2025.0040